Paper I

Yongjia Song and Sigbjørn Grønås (2007)

Downscaling experiments with a global atmospheric model – systematic errors and added value.

Downscaling experiments with a global atmospheric model – systematic errors and added value

Yongjia Song[1], Sigbjørn Grønås[2]
1 Bjerknes Centre for Climate Research, University of Bergen, Norway
2 Geophysical Institute, University of Bergen, Norway

Abstract

Within the climate research community continuous activity is accomplished to improve the coupled global climate models for systematic errors in the general circulation. Generally, improvements are obtained by increasing the spatial resolution and improving the parameterisation of sub-scale processes. In this paper we have made experiments with the atmospheric part of the climate model BCM (Bergen Climate Model) with higher resolution than normally afforded for coupled integrations. Runs have been made for around 15 years using observed surface forcing from reanalyses (ERA40). Comparison of the results with observed evidence from ERA40 shows that some systematic errors are reduced with higher resolution, e.g. more realistic storm tracks in the Norwegian and Barents Seas. A serious systematic error was, however, revealed for all resolutions: too strong baroclinicity at mid-latitudes, in particular upstream of the Icelandic Low. The excessive baroclinicity contributes to stronger westerlies than observed and a too deep Icelandic Low when the resolution is sufficient for a proper description of individual extratropical cyclones. Over the Arctic the atmosphere was found to be too warm in lower troposphere due to insufficient representation of the Artic inversions. The experiments were also performed in order to examine strategies for dynamical downscaling in Arctic of normal course resolution coupled integrations. Strong arguments were found for application of a global atmospheric model with focussed resolution for this region on the expense of lower resolution on the opposite side of the globe. However, the value of dynamical downscaling must be weighed up against the level of systematic errors in the coupled model. As always, reduction of systematic errors in AOGCMs remains a priority for the climate modelling community.

1. Introduction

Climate models that couple atmosphere and ocean (Atmospheric-Ocean-General-Circulation-Models; AOGCMs) are the primary tool used for understanding of past climate variations and for future projections. The climate models are steadily developed through improved spatial resolution and improvements in numerical schemes and parameterisations. The climate model at Bjerknes Centre for Climate Research (BCCR), called Bergen Climate Model (BCM; Furevik et al. 2003), is one of several internationally recognised climate models. The model is basically a coupling of the atmospheric climate model ARPEGE developed at Meteo-France (Déqué et al., 1994, 1998; Déqué and Piedelievre, 1995) built on the numerical integration scheme used in weather prediction model used at the EWMWF (IFS), and the ocean model MICOM (Bleck et al. 1992). The coupling is made trough the coupler OASIS (Terray et al., 1995). Special for BCM is a flexible coupling, where the ocean grid might be chosen independently of the grid of the atmosphere (Furevik et al., 2003), and an advanced module for sea-ice (Drange, 1999). Like other models BCM is steadily being improved -

ARPEGE through cooperation with Meteo-France - and is now one of several climate models that are run without ocean flux adjustment (methods to remove long-term drift in the simulated climate, see IPCC, 2001). However, some long-term drift of climate variables still remain in control runs (Nils Gunnar Kvamstø, personal communication).

Generally, the society needs reliable knowledge of future climate change on a regional and even a local scale, in particular risks for extreme weather events. AOGCMs remain the primary source for regional information on possible future climates. However, the spatial resolution of the climate models is still modest and generally too course for an accurate description of regional and local weather. Above all, extreme weather like extreme wind and extreme precipitation are generally inadequately described. There is a general goal to increase the resolution of AOGCMs to that of modern weather prediction models for the atmosphere and to even better resolution for the ocean where Rossby deformation radius is shorter than in the atmosphere. Limitation in the resolution is set by the computing capacity of the super-computers which steadily become faster, however. The resolution of BCM will be enhanced according to increases in the computing facilities provided by the Norwegian Research Council. It should be emphasised that scientific efforts to increase the resolution involve extensive work to improve and adapt sub-scale parameterisations of physical processes accordingly.

The climate of a region is determined by the interaction between regional forcings and atmospheric and oceanic circulations that occur at a range of spatial and temporal scales. Examples of regional and local scale forcings are those due to complex topography, land-use characteristics, land ocean contrasts, snow, sea-ice, and distribution of ocean currents. Moreover, teleconnection patterns such as those associated with North Atlantic Oscillation (NAO) (e.g. Hurrell, 1995) can strongly influence interannual and decadal variability, and the regional climate responses to forcing. The difficulties related to the simulation of regional climate and climate change, are thus quite apparent.

In several ways climate research communities try to increase the climate information provided by the global models towards more details on regional and local scales. We call this activity downscaling, and certain downscaling techniques exist to increase the regional information. Empirical methods have been developed where measured relations between large-scale flow patterns and local weather form the basis (IPCC, 2001, e.g. Cannon and Whitfield, 2002; Blenckner and Chen, 2003). The main downscaling method is, however, dynamical downscaling, where additional details are extracted using a climate model of the atmosphere with higher resolution than in AOGCMs. In this way both regional forcing from the surface and individual weather systems will be better described. Downscaling models are normally run for time slices of some decades for present and future projections with surface forcing - sea surface temperature (SST) and sea-ice distribution – from observations or from projections from AOGCMs.

Different approaches exist to dynamical downscaling. Typically a regional atmospheric climate model (Regional-Climate-Model; RCM) will be used. Such a model covers a limited geographical area and takes its lateral boundary conditions from a run with an AOGCM. While a horizontal grid length of an AOGCM might typically be 300 km, a

common grid length of a RCM is 50 km or less. RCMs will have a much better description of coastlines and topography and a much better description of mesoscale weather phenomena normally associated with extreme weather. When relatively small geographical areas are chosen for a RCM, the large-scale flow will be similar to that from the AOGCM used as lateral boundary conditions. When larger areas are used, results from a RCM might in principle give a different large-scale flow than that of the AOGCM. However, RCMs are not able, nor intended to correct the large-scale errors made by the global model.

Another computationally more expensive downscaling method is to use a global climate model for the atmospheric (Atmospheric-General-Circulation-Model; AGCM) with better spatial resolution than in the atmospheric part of AOGCMs. The atmospheric model is then typically run with a horizontal grid size of 100 km. Since better resolution normally means better representation of the forcing from the surface and reduced computational errors in the model, downscaling with global models normally reduces systematic errors present in AOGCMs, for instance a better positioning of jets at the top of the troposphere and better description of individual extratropical cyclones. Global atmospheric models might often be run with a variable horizontal grid, where the resolution is increased in a certain area, e.g. Europe, with a coarser resolution elsewhere on the globe. The advantage with this approach is less computation requirements than for models with a uniform high resolution. Both the atmospheric and the oceanic part of BCM have this ability to focus the resolution in an area. Downscaling experiments for the atmosphere using ARPEGE have been done by Déqué and Piedelievre (1995) Gibelin and Déqué (2003). The focussing of the resolution is here done by stretching the horizontal coordinates and we denote such models Stretched-Atmospheric-General-Circulation-Models (SAGCM).

The dynamical downscaling methods mentioned here are further reviewed in Section two. Climate modelling and downscaling in Arctic is exceptionally challenging because of numerous nonlinear interactions between and within atmosphere, cryosphere, ocean and land. Section two includes approaches to downscale the climate in Arctic using regional models that couple atmosphere, sea ice and ocean.

BCCR wants to exploit the benefit of dynamic downscaling using ARPEGE, the global atmospheric part of BCM. As a step towards a downscaling strategy we have made some experiments with ARPEGE as an AGCM and a SAGCM with higher horizontal resolution than hitherto used in BCM. The focussing of the resolution using ARPEGE as a SAGCM is made for Arctic. In this way downscaling for Arctic is emphasised. The experiments might also be considered as a step in BCCRs ongoing activity to reveal and reduce systematic errors in integrations with BCM. The experiments are made using SST and distribution of sea-ice from GISST (Global Sea Ice and Sea Surface Temperature) reconstructed datasets, integrations for around 15 years have been made. The following resolutions have been used: T63 which is a resolution commonly used in the atmospheric part of the coupled BCM and which correspond to a horizontal grid length of 2.875 degrees, T159 which correspond to a grid length of 1.1 degrees and T319 which correspond to a grid length of 0.5 degrees. In addition we have made a similar experiment with stretched coordinates with resolution denoted T159S, where the number of

horizontal grid points is the same as in T159, but where the grid resolution in Arctic is 0.5 degrees – similar to T319 - and reduced towards that of T42 over the Antarctica. In Section three the experiments are described in detail. The results of the experiments are evaluated against ERA40 reanalyses which are available in T159.

Evaluation of our experiments might be made in different ways. Boer (2000) distinguished between the following three evaluation categories: evaluation of the morphology of climate, including spatial structures of means, variances; budgets, balances and cycles in the climate system; and process studies of climate. In this paper the evaluation is according to the first of these categories. In Section four we discuss systematic errors in the experiments concentrating on the sea level pressure, baroclinicity expressed by the thickness 500 – 1000 hPa, 500 hPa height and storm tracks - estimated from band-passed standard deviations (Blackmon, 1976) - for mid-latitude and higher northern latitudes pointing to changes – improvements and deteriorations - when resolution is increased. In Section five we discuss the downscaling results for Arctic concentrating on the representation of extreme precipitation and wind. Concluding remarks are made in Section six concerning systematic errors in the experiments with ARPEGE relative to resolution and a downscaling strategy for BCCR.

2. Dynamical downscaling methods

As mentioned, AOGCMs constitute the primary tool for simulating the global climate system. They are also the main tool to study the processes responsible for maintaining the general circulation and natural variability, and its response to external forcing. Since there is a need to integrate the complex, computer-demanding AOGCMs for many centuries, horizontal resolutions of the atmospheric components of the AOGCMs range from 400 km to 125 km, with 300 km a typical value.

Depending on the resolution, AOGCMs have some ability to simulate current regional weather and climate. Spread among the model results is to a large extent the result of natural variability and different responses of models to a prescribed forcing. A large spread in a region might be related with important feedbacks and be a signal of large uncertainties. Small spread in an ensemble of projections does not necessarily grant small uncertainty of the projected climate changes, but might merely reflect that the models have similar errors. The response in simulations with all known forcing within the last century can, however, be validated against the observed response of the climate system. Results from such integrations will constrain the likelihood of future climate change projection (Stott et al., 2006).

As already explained, dynamical downscaling is achieved through high-resolution numerical climate models for the atmosphere that use needed boundary conditions from AOGCM simulations. The models are atmosphere-only climate models, of uniform or variable horizontal resolution, and nested regional RCMs. Dynamical downscaling models have the potential to describe mesoscale nonlinear effects and extreme values of parameters such as surface wind and precipitation. Confidence in these methods to realistically downscale future climates comes from their ability to reproduce widely varying climates around the world with the same model.

AGCMs

AGCMs are run with finer meshes than the AOGCMs. They might include similar interactive land-surface processes as in AOGCMs, but SST and sea-ice are prescribed by interpolation of results from AOGCMs or from observations (analyses) when present day or historic climate is simulated. A resolution of 100 km is the present standard, less than 50 km will be likely in the near future (Déqué and Gibelin, 2002; Govindaswamy, 2003). Some computers, in particular the Japanese Earth Simulator, now allows for even higher resolutions (Yoshijaki et al., 2005)

Downscaling results using AGCMs with typical resolution agrees better with observations than current AOGCMs, i.e. the systematic errors in the atmosphere are reduced. A notable improvement is better description of extratropical and some extent even tropical cyclones. Since the topography and coastlines are better resolved, the mountain flows, e.g. orographic precipitation, become more realistic. The effect of increased resolution might, however, vary significantly with region (Duffy et al., 2003).

Since there is no feedback between atmosphere and ocean, climatic variability could be distorted when downscaling with AGCMs (Bretherton and Battisti, 2000; Douville, 2005; Inatsu and Kimoto, 2005). Due to the difference in the resolution between AGCMs and AOGCMs, their large-scale climate responses might be different. A question of consistency of the oceanic lower boundary conditions with the atmospheric forcing might appear (May and Roeckner, 2001; Govindasamy et al., 2003).

We have already mentioned variable-resolution AGCMs as an alternative to models with uniform grid lengths (Déqué and Piedelievre, 1995; Fox-Rabinovitz et al., 2001; McGregor et al., 2002; Gibelin and Déqué, 2003). This approach is attractive as it permits to achieve a regional increase of resolution while retaining the full interaction of all regions of the globe. Numerical errors due to stretching have been shown to be small when using modest stretching factors (e.g., Gibelin and Déqué, 2003). The models results show some ability to capture finer scale details than models with coarser uniform resolution, while retaining global skill similar to simulations with uniform resolution with the same number of grid points.

RCMs

In the regional climate models (RCMs) time-varying atmospheric fields (winds, temperature and moisture) are supplied as lateral boundary conditions, and SST and sea-ice are supplied as lower boundary conditions. If the integration area is relatively small, the lateral boundary conditions exert sufficient control to keep the large-scale flow consistent with the driving large-scale atmospheric circulation. Details of the regional climate are obtained as a result of better resolution, combined with suitable parameterisation of subgrid-scale physical processes and improved surface forcings from orography, land-sea contrast and land use. The first to demonstrate successful results were Dickinson et al. (1989) and Giorgi and Bates (1989). Recently a two-way nested RCM has been developed (Lorenz and Jacob, 2005) that allows feedback from the RCM onto the larger scales. RCMs are now being coupled interactively with other components

of the climate system, such as regional ocean and sea ice (e.g., Maslanik et al., 2000; Döscher et al., 2002; Rinke et al., 2003; Debernard et al., 2003; Schrum et al., 2003; Meier et al., 2004; Rummukainen et al., 2004), hydrology, and some work has been initiated with interactive vegetation (Gao and Yu, 1998; Xue et al., 2000).

The difficulties associated with the implementation of lateral boundary conditions in RCMs are well documented (e.g. Warner et al., 1997). In fact, mathematically nested models represent an ill-posed boundary-value problem (e.g. Staniforth, 1997). The control exerted by lateral boundary conditions on solutions generated by RCMs appears to vary with the size of the computational domain (e.g. Rinke and Dethloff, 2000), as well as location and season (e.g., Caya and Biner, 2004). In some applications, the flow developing within the RCM domain may become incoherent with the driving boundary conditions. This may have an impact on the results (Jones et al., 1997), however, it is believed that the effect is small (Caya and Biner, 2004).

It has been demonstrated that RCMs generate meaningful fine-scale structures that are absent in larger scale AOGCM results. This means that climate statistics of small-scale features can be recreated with the right amplitude and spatial distribution, even if these small scales are absent in lateral boundary conditions (Bjørge et al., 2000; Denis et al., 2002, 2003; Antic et al., 2005; Dimitrijevic and Laprise, 2005). Thus RCMs can contribute added value at small scales to climate statistics when driven by AOGCMs that give accurate large scales. However, de Elía et al. (2002) found that nested models are incapable of maintaining deterministic temporal coherence of small-scale features (at the right place at the right time) beyond a day or so, even if these were present initially and in the lateral boundary conditions. Teige (master thesis 2005, Department of Geophysics, University of Bergen) on the other hand, found no change in the deterministic coherence of small-scale features over southern Norway in runs with a high resolution limited area model over a month, using ECMWF numerical analyses as lateral boundaries.

RCMs have been successfully applied to several regions around the world, to simulate recent past climate as well as climate-change projections. Using reanalyses of the atmosphere Vidale et al. (2003) have shown that RCMs have skill in reproducing interannual variability in precipitation and surface air temperature. Typical RCM grid distance for climate-change projections is around 50 km, although some climate simulations have been performed at higher resolutions, with meshes such as 20 km. Recently climate-change projections have been completed on the Earth Simulator with a 5 km mesh non-hydrostatic RCM over for East Asia (Kanada et al., 2005; Yoshizaki et al., 2005), for 10 years of June and July, driven by the outputs of a 20 km AGCM. Since the ability of RCMs to simulate the regional climate depends strongly on the realism of the large-scale circulation that is provided at the lateral boundary conditions (e.g., Pan et al., 2001; de Elía et al., 2006), reduction of errors in AOGCMs remains a priority for the climate modelling community.

Approaches towards downscaling with coupled models

The Arctic climate is complex due to numerous nonlinear interactions between and within the atmosphere, cryosphere, ocean, and land. Sea ice plays a crucial role in the

Arctic climate, through the albedo-temperature feedback and feedbacks associated with the heat flux through the ice and with clouds. In both models and observations, the interannual and decadal climate variability has a maximum in high latitudes (Räisänen, 2002; Johannessen et al., 2004; Bengtsson et al., 2004; Sorteberg and Kvamstø, 2003). The complexity of Arctic climate includes many processes that are still poorly understood and thus continue to pose a challenge for climate models (ACIA, 2005). In addition, the evaluation of simulations in the Arctic is made more difficult by few available observations, and different data sets might differ considerably (Serreze and Hurst, 2000; Liu et al., 2005; Wyser and Jones, 2005; ACIA, 2005). One example is precipitation measurements which are notoriously problematic in cold environments (Goodison et al., 1998; Bogdanova et al., 2002).

A few RCMs have bee applied to Arctic. When driven by lateral boundary conditions from reanalyses and observed sea-ice, RCMs tend to show smaller temperature and precipitation biases in Arctic compared to GCMs. This indicates that sea ice simulation biases and biases originating from lower latitudes contribute substantially to the contamination of GCM results in the Arctic (e.g., Dethloff et al., 2001; Wei et al., 2002; Semmler et al., 2005). But even with observed lateral and lower boundary conditions, there can be considerable across-model scatter in the simulations (Tjernström et al., 2004; Rinke et al., 2006).

Because of large errors in AOGCMs, the value of traditional dynamical downscaling, using atmospheric models only, has been questioned (e.g. Rinke and Dethloff, 2000). As indicated above, some research communities have developed limited area coupled models with particular emphasis on interaction through sea-ice. Some of the models are applied for the Arctic (Maslanik et al., 2000; Rinke et al., 2003; Debernard et al., 2003; Mikolajewicz et al., 2005; Røed and Debernard, 2006). The main goal with these developments is to get at a better representation of sea ice than in global climate models. The models are still in their infancy, and successful decadal integrations for present day climate, showing increased climate information for Arctic compared to downscaling with a atmospheric model only, have not yet been demonstrated. The models are of course computationally very expensive. Coupled global climate models like BCM, offer an alternative to limited area coupled models since both resolution might be focussed for both atmosphere and ocean. There is also a possibility to relax the regional results to reanalyses, ocean climatology or other global patterns that are available.

3. Set-up of experiments

The ARPEGE/IFS (Action de Recherche Petit Echelle Grande Echelle / Integrated Forecast System) model was developed as a forecast model in a joint effort between Meteo-France and European Centre for Medium range Weather Forecasts (ECMWF; Déqué et al. 1994, 1998; Déqué and Piedelievre 1995). Later the model was also expanded and adjusted to the needs for a community climate model for research purposes. The model is described in more detail in Déqué et al. (1994).

ARPEGE is a spectral model with Fourier components along longitudes and Legendre polynoms along latitudes. The horizontal resolution for the dynamical fields is given with

a triangular truncation in the spectral components. The grid structure used in ARPEGE give a uniform resolution on the sphere – Gaussian grid - with no converging of the grid-points towards Arctic (Hortal and Simmons 1991). In the studies presented here a spectral resolution of T63 means that the dynamical fields are expressed with a cut-off at wave number 63 in the Fourier components. The number of grid points will then be 64 between the poles and 128 grid points along the equator. Reduction of the grid towards the pole (so-called Gaussian grid) gives a total of 6232 grid points over the globe. A so-called linear grid is used, which means that linear terms in the dynamical equations are resolved in T63, while non-linear terms (advection) and local rates of change in the variables due to diabatic and sub-grid effects are computed in with lower truncation. We note that with the linear approach, topography is resolved in T63. For T63 the grid used for advection and physical parameterisations has a grid length of 2.8 ° (T42 in a non-linear grid). The output from an integration with T63 – should be denoted T_L63, where L denotes a symbol for the linear grid.

The vertical resolution is given as a hybrid vertical coordinate, which means a weighting of sigma-coordinates and pressure-coordinates in such a way that the model surfaces follow the terrain at the ground (sigma-coordinates) and pressure surfaces at higher levels. In our experiments the default configuration of ARPEGE has been used with 31 vertical layers, 21 layers in the troposphere and 10 in the stratosphere. The spacing between the levels is most dense close to the ground with a vertical spacing of a few 100 meters near the ground.

In all experiments initial conditions and surface forcing – SST and sea-ice from GISST (Global Sea Ice and Sea Surface Temperature) reconstructed datasets. No external radiative forcing have been applied and the level of greenhouse gases and aerosols are kept constant (353 ppm (part per million volume) for CO_2, 1.72 ppm for CH_4 and 310 ppb for N_2O, 280 ppt for CFC-11, 484 ppt for CFC-12). Version of 3 of ARPEGE has been used.

Four experiments have been made with the same model configuration, same number of vertical layer, but with different resolution:

1. Experiment T63, which is run with linear grid T63 corresponding to a grid distance of 2.8 °. This resolution is the standard resolution used for BCM, e.g. in control runs without external forcing (Furevik et al. 2003). T63 is run for 47 years starting 24 January 1950, i.e. longer than for the other experiments. However, the results of the experiments are shown for a period of 15 years starting 24 January 1978.

2. Experiment T159, which again means a run with linear grid T159 corresponding to a grid distance of 1.1 °. T159 is run for 13 years stating 24 January 1978.

3. Experiment T319, a run with linear grid T319 corresponding to a grid distance of 0.5 °. T319 is run for 11 years starting 24 January 1978.

4. Experiment T159S where the coordinates are stretched to that of T319 in Arctic on the expense of lower resolution, T42, over Antarctic. T159S is run for 15 years starting 24 January 1978. The number of grid points is the same as in T159. The stretching is given by a stretching factor of 2.0, which in our case means that grid distance increased from 0.5 °in Arctic to 1.5 °.

The distribution of the grid points in the different resolutions is shown in Figure 1 for the northern hemisphere north of 30 ° N. The results are compared to ERA40, which is available in T159 corresponding to a grid length of 1.1 °. Although the length of the experiments varies a little, we make mean values over the integrated period and compare with means from ERA40 over 15 years (starting 24 January 1978).

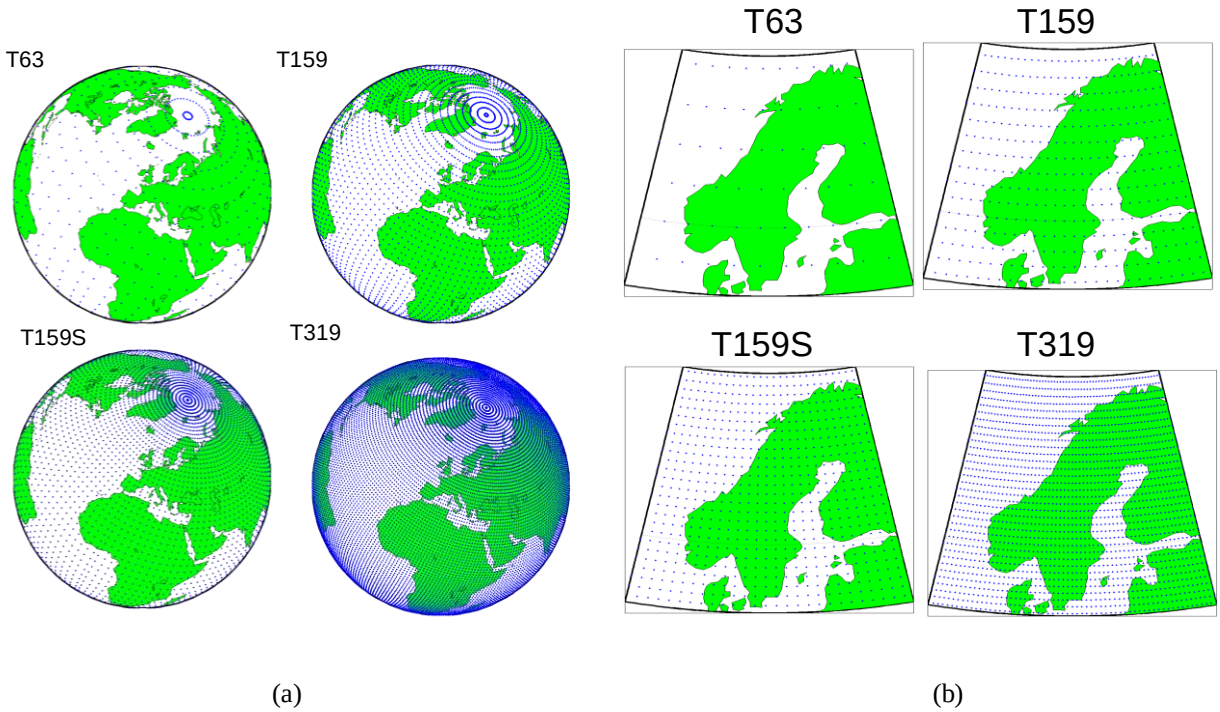

Figure 1. Distribution of grid points horizontally in the different experiments. a) A large area. b) Scandinavia.

4. Systematic errors with increased resolution

The atmospheric part of coupled climate models (AGCMs) have been evaluated following the AMIP protocol (Gates, 1992; Gates et al., 1998; PCMDI, 2004), which stands for experiments with observed (analysed) sea surface temperature and sea ice over recent decades. More than a decade ago, several climate centres carried out such AMIP experiments, and the output remains archived at the Program for Climate Model Diagnosis and Intercomparison (PCMDI). Our experiments are similar to such AMIP experiments where model output from several models has been compared with observations, such as reanalyses. We have results from experiments with one model, and the results will be compared with ERA40 reanalyses only. Since no ensemble of experiments have been made and since the time slice is rather short due to lack of

computer capacity, we will not study temporal variations, but concentrate on systematic errors – mean differences to ERA40 - for vital parameters. In addition, we concentrate on the winter season. Since a downscaling strategy for Arctic is part of the objective, we will concentrate on the northern hemisphere with emphasis on mid and high latitudes. We will first look at mean values of sea surface pressure (4.1), then move on to thickness 500 – 1000 hPa, expressing the baroclinicity, and the height of the 500 hPa surface (4.2). In 4.3 we describe the variability as expressed by certain standard deviations relevant for storm tracks, and a discussion of the results is found in 4.4.

4.1 Systematic errors in SLP

On the resolved scales of the experiments the atmosphere is hydrostatic, with the consequence that the pressure at the surface is the weight of the atmosphere above, which again is determined by the temperature distribution vertically. In weather forecasting the surface pressure is normally reduced to mean sea level to obtain the mean sea level pressure (SLP). The accuracy in this procedure – built on extrapolation of the temperature - is very high for low topography. However, for high topography like the top plateau of Greenland, mean sea level pressure has little meaning. However, in order to get a continuous field of SLP, extrapolation to sea level is made for high mountains, using model temperatures above the mountain surface.

In weather forecasting at mid and high latitudes, it is well known that the distribution and evolution of SLP is the principle single variable to monitor. In the process of evaluating a models ability to represent the observed climate, we claim that the distribution of SLP, e.g. averages and standard deviation over seasons and years, is also the principle parameter to evaluate. An accurate distribution of SLP is a convincing indication of an accurate description of the general circulation, which on synoptic and planetary scales at mid and higher latitudes is closely connected to temperature and wind through geostrophic relations. On the contrary, large errors in the climatic distribution of SLP are serious indications of vital errors in the general circulation of the atmospheric climate model.

Figure 2 shows mean SLP for northern hemisphere from the subtropics to the North Pole in winter (DJF) for the four experiments together with the same field from ERA40. Figure 3 shows the difference in SLP between the experiments and SLP in ERA40. Since realistic surface forcing from GISST has been used in the experiments, the mean values should be close to those in ERA40. However, the chaotic nature of the dynamics of the atmosphere, that might cause some differences in interannual and decadal variation between the experiments, should be born in mind.

All the experiments show the well known climatological large-scale pressure variations: the subtropical highs, i.e. the Azores High, the Pacific/North-American High, the Icelandic and the Aleutian Lows, and the Sibirian High. In this way vital characteristics of the general circulation are present in a realistic way. There are, however, significant differences between the experiments in terms of positioning, shape and amplitudes of these pressure systems and regional details in the pressure distribution in between. In addition to the mentioned structures, we will focus on the pressure distribution over

Arctic, which is dominated by a ridge as an extension from the Sibirian High towards Arctic and the ridge over Rocky Mountains (see SLP for ERA40 in Figure 2).

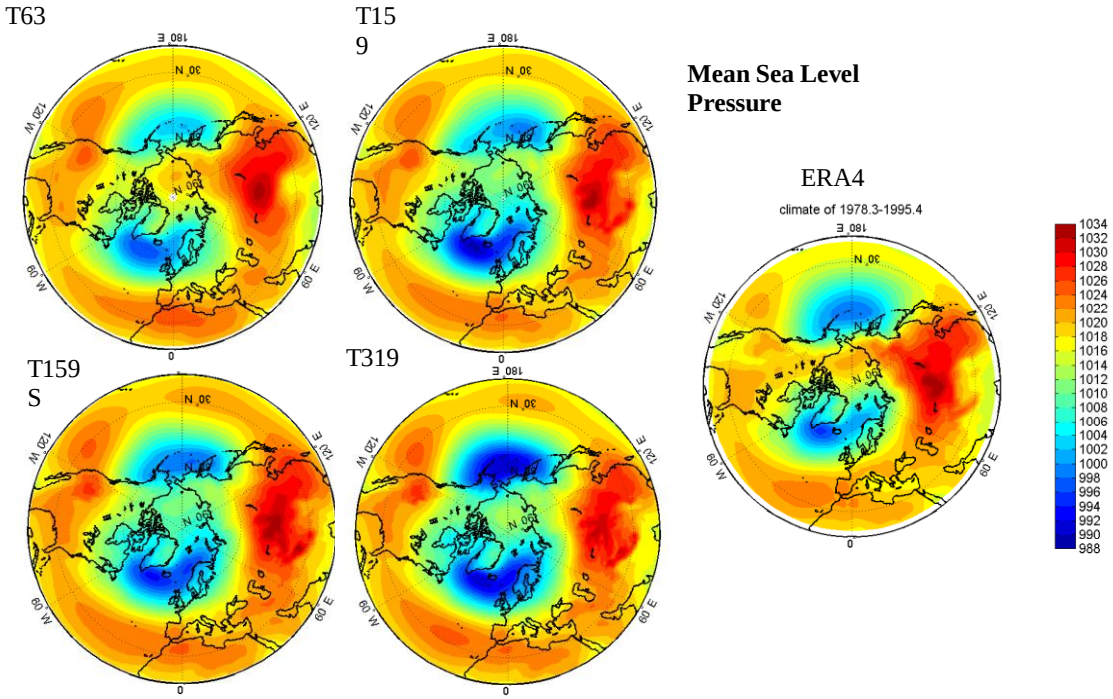

Figure 2. Mean SLP in winter (DJF) for ERA40 and the four experiments and ERA40. The isobar interval is 2 hPa.

It is interesting that the lowest resolution (T63) in several ways shows smallest systematic errors, defined as the difference between experiments and ERA40. The depth of the Icelandic Low is nearly as in ERA40 (minimum of 998 against 997 hPa in ERA40). Also the amplitude of the ridge in interior Arctic is nearly correct, the shape is too broad, however. On the other hand, the Aleutian Low is too shallow in T63 (1003 against 1001 hPa). The sub-tropical highs are stronger in T63 than in ERA40 (about 2-3 hPa) and extend too far eastwards over land.

Despite rather correct amplitudes of the main systems, there are severe errors in T63. The Icelandic low is positioned a little south of its position in ERA40, and the pressure field over Northern Europe is too westerly oriented with too strong gradients (south-north). The trough extension from the Icelandic Low northeastwards into the Barents Sea is too weak, and the trough southwards from the Baltic is too strong and too broad. In this way we find relative large errors over Europe. The amplitude of the mentioned ridge in Arctic is too weak toward the ridge over Rocky Mountains. Figure 3 shows a circumpolar band of negative errors, with the largest amplitudes from the Icelandic Low over Europe and Siberia. Over North-America this band is further to the north, from the Bering Strait to western Canada. Large positive errors south of the Aleutian Low illustrate a too small scale of this low. We also notice a positive anomaly over Arctic.

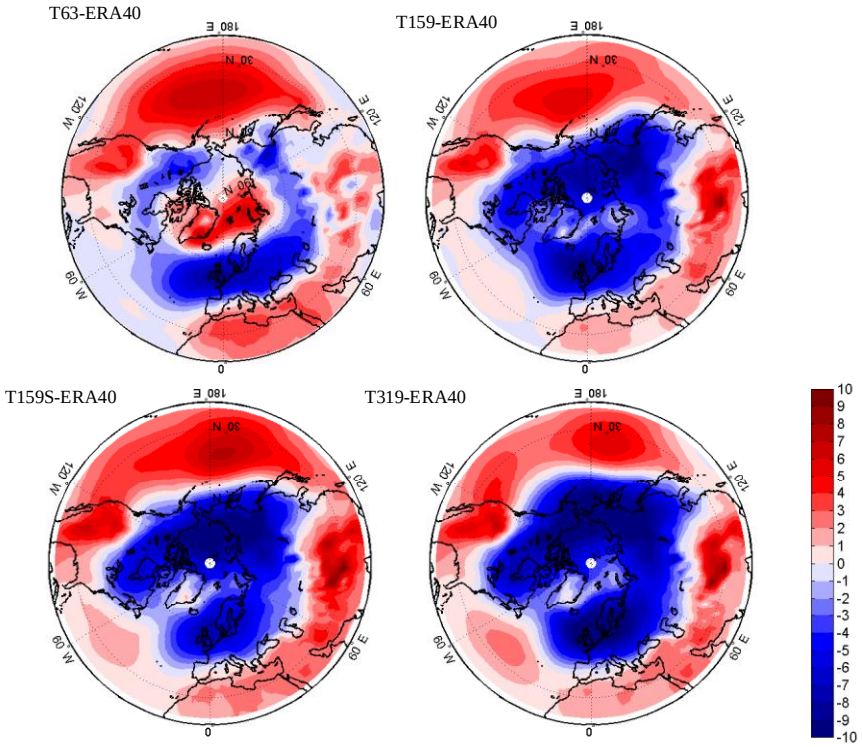

Figure 3. Difference of mean SLP in winter (DJF) between experiments and ERA40. Contour interval is 1hPa.

An increase in the resolution to T159 gives relative large changes in the distribution. The Icelandic Low becomes considerably stronger than in ERA40 (minimum of 991 hPa against 997 hPa), but has a better position and a better shape than in T63. The Aleutian Low is also stronger and nearly as in ERA40. The Arctic ridge is much weaker than in ERA40 and in T63, but the shape seems to be better. At the same time the sub-tropical highs are too strong, much as in T63, but the Azores High is extended slightly westwards, towards its correct position. We find a similar circumpolar band of negative errors like in T63. The strong sub-tropical highs and the pressure deficit in Arctic, indicate a large-scale error over the northern hemisphere, negative at higher latitudes.

In T159 several vital structures on regional scale, such as those related to Europe mentioned for T63, are in better agreement with ERA40. First of all the trough extension from the Iclandic Low towards the Barents Sea is better simulated. The southward trough from the Baltic Sea has also a shape in better accordance with that in ERA40. The pressure gradients over northern Europe are still too westerly and too strong, but a little better than in T63.

The Siberian High is a dominating structure in all experiments as well as in ERA40. The amplitudes are difficult to evaluate since the position of maximum pressure is over high mountains. The main error compared to ERA40 is found in the extension of the ridge towards Arctic. For T159 the amplitude of the ridge is far too weak.

An increase of the resolution from T159 to T319 does not change the picture described above very much, except that the Aleutian Low becomes even stronger (minimum 993 hPa against 1001 in ERA40). In addition, the sub-tropical highs now have an even better position over ocean. As with lower resolution, the amplitudes are still too high. Flows over mountains become more realistic, e.g. as expressed with the lee trough west of Greenland which is in good agreement with ERA40.

The experiment with stretched coordinates, T159S, shows the smallest systematic errors in relation to ERA40. The Icelandic is too deep, but not as deep as in T159 and T319. The Aleutian Lows have nearly correct amplitude, position and shape. The extension towards the Barents Sea for the Icelandic Low is much as in T319. The improvement in regional variations over Europe obtained in T159 and T319, are still present in T159S. As in T159 and T319 the amplitude of the ridge in Arctic is too low.

4.2 Systematic errors in thickness 500-1000 hPa and height of the 500 hPa surface

Extratropical cyclones are associated with baroclinic generation, i.e. conversion of available potential energy (APE) of the mean flow to cyclones. In general the cyclones are vigorous downstream of the regions of maximum baroclinicity. According to Hoskins and Valdes (1990) the track of the storms are self-maintained due to diabatic heating maxima caused by the cyclones themselves. In this way enhanced baroclinicity is actively maintained by condensational heating over the storm track entrance region. Lee and Mak (1996) argued that the storm tracks are not completely self-maintained. They showed that enhanced baroclinicity over the storm track entrance region could also be maintained by stationary waves induced by mountains without the need for diabatic heat sources near the storm track entrance regions. According to Chang and Orlanski (1992) the extratropical cyclones start in a region called baroclinic generation zone. They develop eastwards from the baroclinic generation area in a process they called downstream development. They also argued that cyclone developments may be considered as an ensemble of wave packets. This concept was further developed by Chang et al. (2002) who considered storm tracks transients as an ensemble of wave packets with wave growth and decay occurring over all portions of the storm track, and that these waves propagate eastwards. The storm track development may also be illustrated from an energetic point-of-view (Orlanski and Katzfey 1991; Chang and Orlanski 1992; Chang et al. 2002). First, there is baroclinic generation of energy over the baroclinic generation zone. Then eddy energy is dissipated over the downstream area (downstream development) by barotropic conversion, and surface friction over the continents (dissipation).

The Eddy growth rate (e.g. Chang and Orlanski, 1992) is defined as:

$\sigma_{BI} = 0.31*f/N*|\partial \mathbf{V}/\partial z|$,

where f is the Coriolis parameter, N the Brunt-Väisälä frequency ($N^2 = g/\theta(\partial\theta/\partial z)$), z is the vertical distance and $\mathbf{V}$ the horizontal wind vector. The distribution of the Eady growth rate correlates well with regions of high eddy activity (Chang and Orlanski, 1992) and can easily be mapped from output from our experiments. The evolution of the

cyclones is found downstream of the source baroclinic region mapped by the Eady growth rate and thus for baroclinicity.

The Eady growth rate is normally computed as a mean value for the troposphere. The vertical wind shear used in the definition is related to horizontal temperature gradients through the thermal wind relation. In the following we will study the gradients of the thickness between 500 and 1000 hPa as a proxy for the Eady growth. Since the thickness is the mean temperature in the layer, the horizontal gradients of the thickness expresses the vertical wind shear. Our proxy does not include the dependence of the growth rate on the vertical stability expressed by the Brunt-V äis ä l ä frequency N and the variation in the Coriolis parameter. However, N does not vary much between our experiments. Inspection has shown that the gradients in the thickness are well correlated with the Eady growth rate for the troposphere. However, the variation of f should be taken into consideration.

Thickness 500 – 1000 hPa

The mean thickness in the experiments is shown for the winter season in Figure 4 together with the thickness in ERA40, while Figure 5 shows the difference between thickness in the experiments and that in ERA40. In T63 the thickness is too cold (negative differences) in a circumpolar band around a centre over eastern Greenland. The band extends from the Icelandic Low up the Norwegian Sea, over the coast of Sibera to the Bering Strait and over central Canada. Maximum difference is from -60 to -80 m, corresponding to a mean temperature anomaly of -3 to -4 ℃. South of the band we find small positive differences. In this way we find stronger gradients than in ERA40 in the thickness south of the minimum in the circumpolar band. Upstream of the Icelandic Low, south of New Foundland, the increased north-south gradient – representing increased baroclinicity - is 50-60 m over approximately 10 latitudes. Similar increased gradients are found over Siberia and in the Pacific.

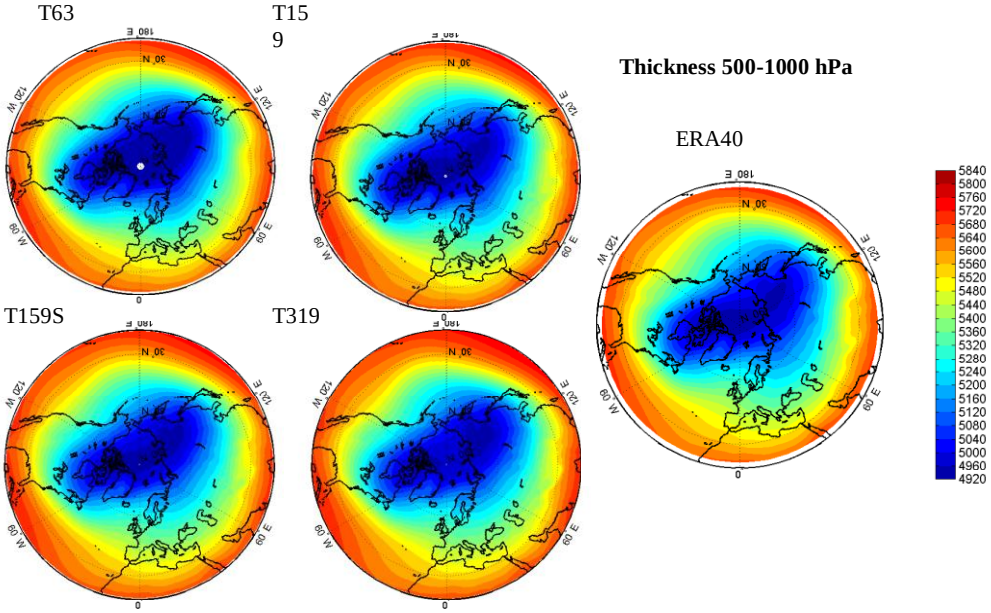

Figure 4. Mean thickness 500 -1000 hPa in winter (DJF) for the different experiments and ERA40. Contour interval is 40m.

Higher resolution gives stronger regional variation in the thickness pattern, and the circumpolar band is broken up in several minima in the difference. In T319 there is a minimum in the difference south of Iceland extending over the Norwegian Sea. Maximum difference is – 50 m. Similar areas with a little smaller amplitude, are connected to the Aleutian Low and found over central USA. The positive differences in south are higher than in T63. Increased baroclinicity represented by increased gradients in the thickness are still found upstream of the Icelandic Low, over Sibiria and in two areas over the Pacific. The increased baroclinicity is slightly smaller in T319 than in T63. In parts of Arctic we now find positive differences, indicating slightly warmer lower troposphere in T319 than in ERA40.

Results from T159 for the thickness is between those in T63 and T319, but closer to T319 than to T63. Differences in thickness for T159S are much as for T319, in particular at higher latitudes.

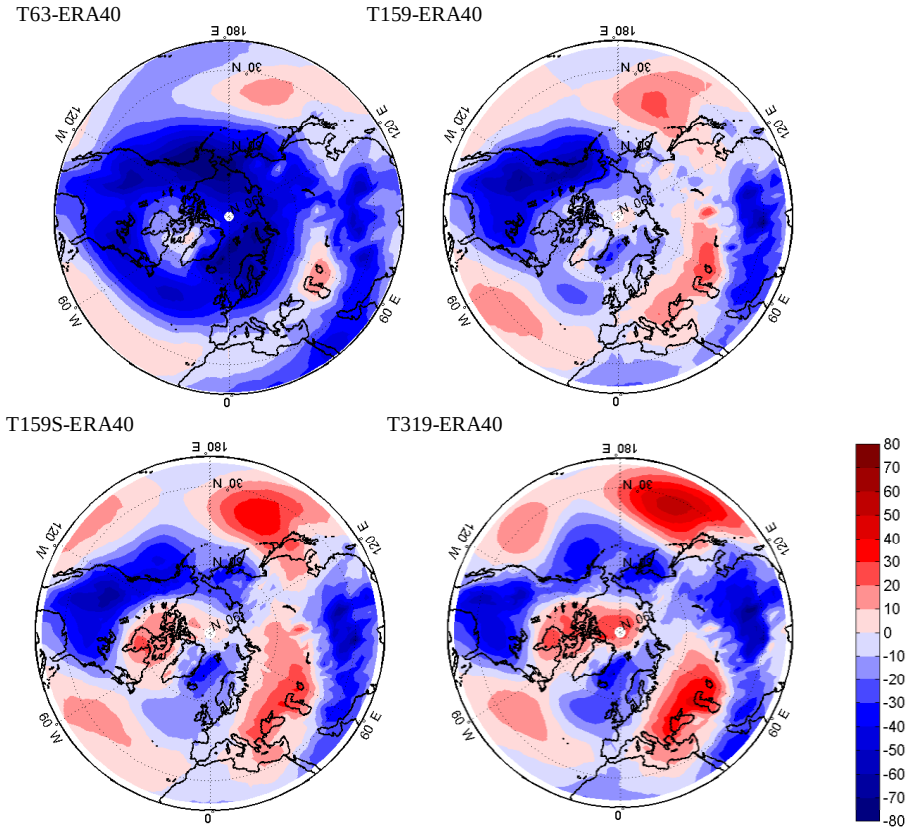

Figure 5. Differences in thickness 500 – 1000 hPa in winter (DJF) between the experiments and ERA40. Contour interval is 10m.

500 hPa height

When the SLP maps are interpreted as geopotential height of the 1000 hPa surface, the height of the 500 hPa surface becomes a sum of the height of the 1000 hPa surface and the thickness. The systematic errors in the height of the 500 hPa surface are then of course the sum of the systematic errors in the height of the 1000 hPa surface and errors in

the thickness. Figure 6 shows the height of the 500 hPa in winter in the experiments and in ERA40 and Figure 7 the difference between the height in the experiments and height in ERA40. In accordance with earlier results, all experiments show a zonal flow with the large-scale troughs east of the main mountains ranges, very much in the same way as in ERA40. In the sub-tropics the heights are too high since both the surface pressure and the thickness were found to be too high. Consistent with the too strong baroclinicity at mid-latitude, the zonal flow at 500 hPa is too strong in the same latitude band. In particular we note that the wind over Northern Europe has a too strong westerly component in accordance with what we found at the surface and in the thickness. As for the thickness, better resolution does not seem to make large improvements in these errors. Better resolution improves the shape of the troughs and the ridges and thus the regional details. Except for the large-scale errors, the distribution in T319 is closest to that in ERA40.

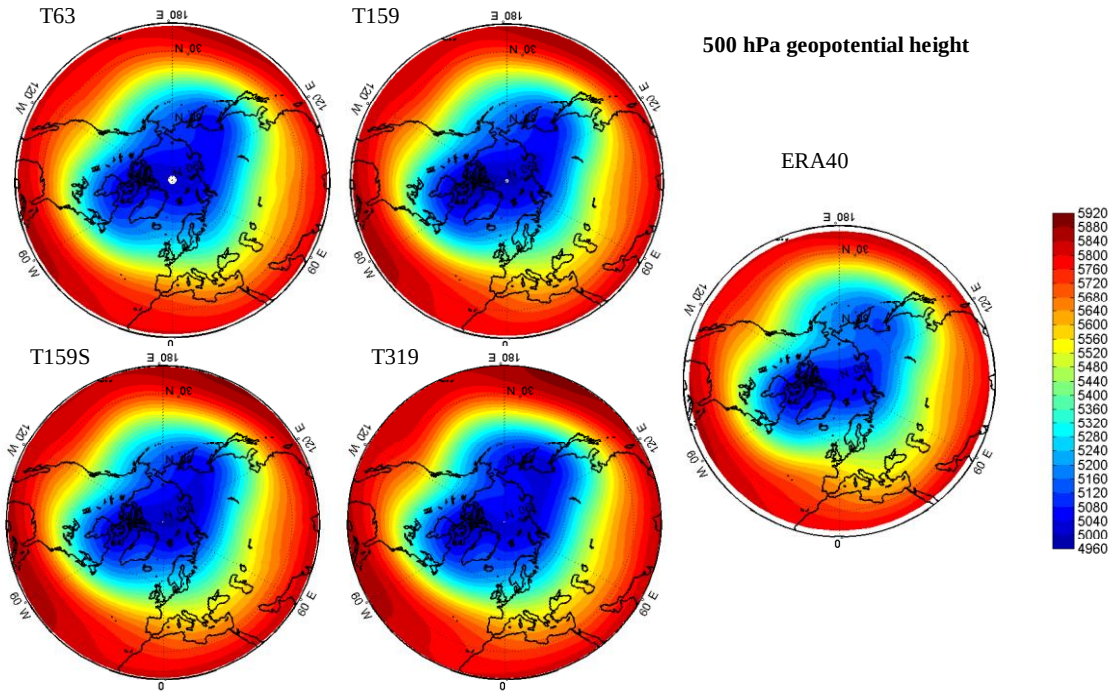

Figure 6. Mean geopotential height at 500 hPa in winter (DJF) in the experiments and in ERA40. Contour interval is 40m.

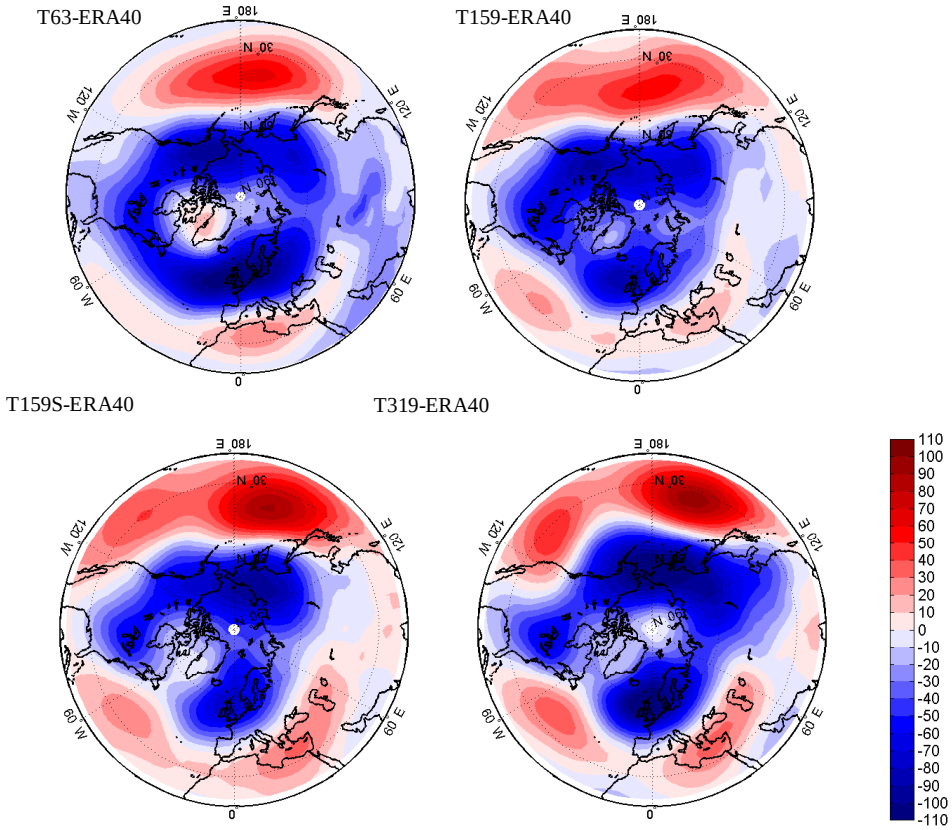

Figure 7. Difference of geopotential height at 500 hPa in winter (DJF) between experiments and ERA40. Contour interval is 10m.

In Arctic, the surface pressure was found to be too low and the thickness too high. Since the effect of the systematic errors in the thickness is stronger than those at the surface, the height of the 500 hPa surface is also too high for Arctic. Higher resolution gives some improvements in this error.

4.3 Storm tracks

We have investigated systematic errors by comparing fields of SLP, thickness 500 – 1000 hPa and height of the 500 hPa surface with the same fields in ERA40. A natural next step in the analysis would be to compare the variability of the same parameters by comparing the standard deviations from the mean fields. We will partly do this, but in order to associate the standard deviation with typical meteorological phenomena, we will do it the way introduced by Blackmon (1976), who isolated typical time scales of the variation by application of certain time filters. Filtering out variations with time scale less than two days and larger than ten days (band-pass filter), extratropical variations stand out. In fact, Blackmon showed that the standard deviation of such band-passed variations give a good proxy for the storm track activity.

Wallace and Blackmon (1983) used this band-filtering technique to analyze the spatio-temporal characteristics of the northern hemisphere daily 500 hPa height for the winters 1962 to 1980. They were able to isolate three time scales. A band-pass filter for periods between two and 10 days picked out baroclinic waves, giving high standard deviation in a

zone above the storm tracks over oceans. A low-pass filter for variation beyond 10 days included variations like blocking of the westerlies. Longer scale variation was studied from 30 day averages. Barry and Carleton (2001) found that the geographical pattern of variance is reasonably constant at time for scales beyond 10 days and that the baroclinic waves do not contribute as much to the total variance as the low-frequency components do. Hoskins and Hodges (2002) argued that "the filtered variance really should be considered as a baroclinic wave-guide since the temporal filtering tended to turn weather systems that on a mean sea-level pressure (MSLP) map moved east-wards and either polewards (cyclones) or equatorwards (anticyclones) into alternating features moving eastwards along the waveguide." Hence, the band-pass variance characterises the storm tracks.

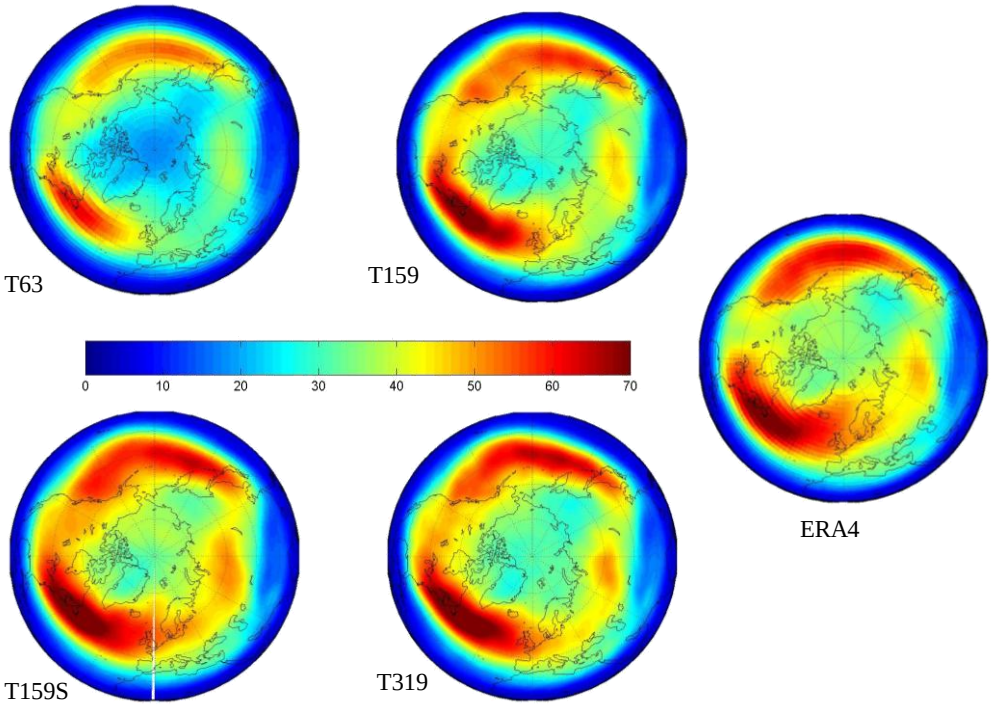

Figure 8. Standard deviation of wintertime geopotential height at 500 hPa (unit m) with band-passed filtering (2-6 days) for the experiments and ERA40.

Figure 8 shows the band-passed (between day 2 and day 6) standard deviation for 500 hPa in winter for the different experiments and ERA40. The amplitude of the standard deviations is generally too low in T63 compared to ERA40. In particular, there is too little low activity in Arctic. Upstream of the Icelandic and Aleutian Lows the storm tracks – as indicated by bands of maximum amplitude – are in the right position. However, these tracks extend towards northern Europe (Britain), while they in ERA40 are stretched up the Norwegian Sea toward the Barents Sea.

Higher resolution gives much more realistic amplitudes of the storm tracks. Clearly there is now more variation in the northern areas and a little stronger storm activity towards the

Barents Sea. However, still the main storm band in the Atlantic is too much directed towards northern Europe and the activity is too small toward the Barents Sea and in Arctic. An increase in the resolution from T159 to T319 does not make large changes. The results with the experiment with stretched coordinates (T159S) are similar to those with high resolution. However, this experiment shows the best performance of the tracks up the Norwegian Sea toward the Barents Sea. We note that the amplitudes upstream of the Icelandic Low are larger than in T63. This indicates that the low amplitude in T63 might be connected to the resolution of the output, which is lower for T63 than for T159 and T159S.

Figure 9 shows similar tracks as in Figure 8, but now for the surface based on SLP. For T63 the amplitudes are closer to those in ERA40 than at 500 hPa. However, the errors are similar to those at 500 hPa with respect to activity over Northern Europe, the Norwegian and Barents Seas and Arctic. We note that the activity in the lee of Rocky Mountains is higher than in ERA40. Inspection of individual weather maps show that the excessive values over mountains like the Rocky Mountains is related to the extrapolation method of the pressure down to sea level. In ARPEGE we find large variations that by no means are connected to similar variations in the surface wind. This means that the variations above high mountains are false and should be ignored.

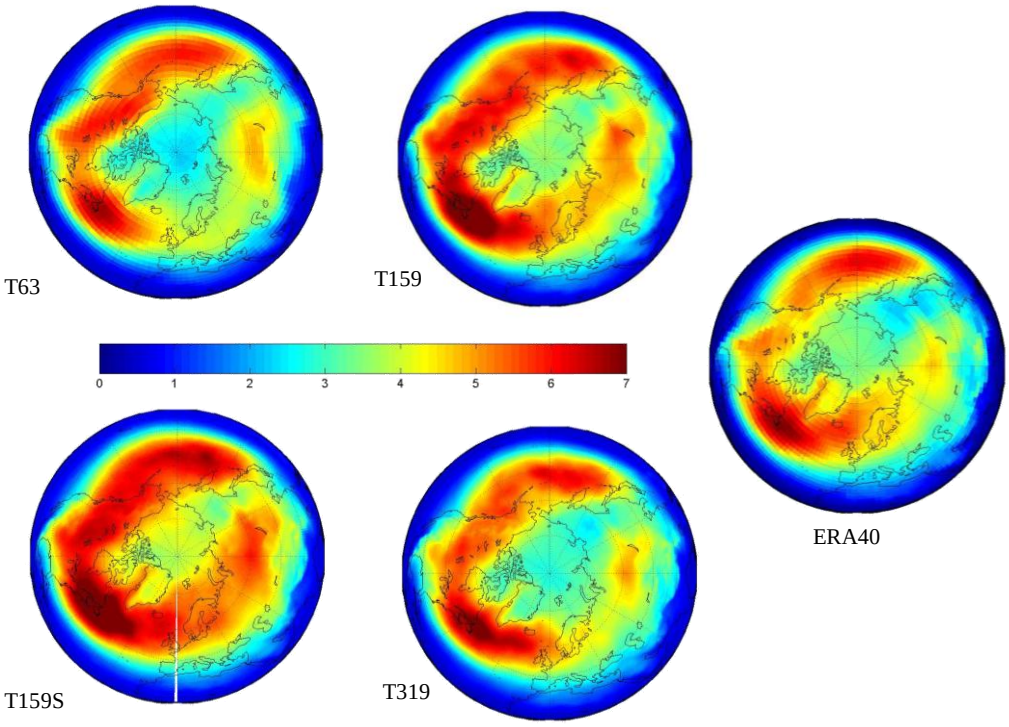

Figure 9. Standard deviation of wintertime geopotential height at 1000 hPa (unit m) with band-passed filtering (2-6 days) for the experiments and ERA40.

Going to higher resolution (T159), the amplitudes become a bit stronger than in ERA40, in particular in the main band upstream of the Icelandic Low. Compared to the results for 500 hPa, there is more low activity in the Norwegian Sea, but still not as much as

observed. The activity in Arctic is about right, however, the activity in the lee of the Rocky Mountains is far too high. Increased resolution to T319 does not make large changes. Also T159S shows similar results. Again, there is more activity up the Norwegian Sea than in the other experiments.

4.4 Discussion

Improved resolution gave simulations in better agreement with observations as expressed with ERA40. However, some systematic error remained. The main error identified is too strong westerlies at mid-latitudes, in particular over Europe. The errors were present both at the surface and in the thickness 500 – 1000 hPa in all experiments. The excessive wind from west is also seen in Figures 10 and 11 showing zonal means of the zonal wind component – vertically and from equator to the north pole - and differences in this quantity between experiments and ERA40 respectively. We see that the mean zonal polar jet is well simulated, but the maximum wind speed is a little less than in ERA40 (about 2 ms^{-1}). However, the wind is too strong from the northern flank of the jet core and down to the surface. The strongest positive error is found between 40 and 50 °North (from 5 to 7 ms^{-1}), and a little bit further south for T63 than in the rest of the experiments. The errors in the stratospheric polar vortex are larger than the errors in the troposphere. We see that the vortex has a larger meridional extension than observed with too strong westerlies at mid-latitudes and too weak winds at higher latitudes. The errors are similar in all the experiments.

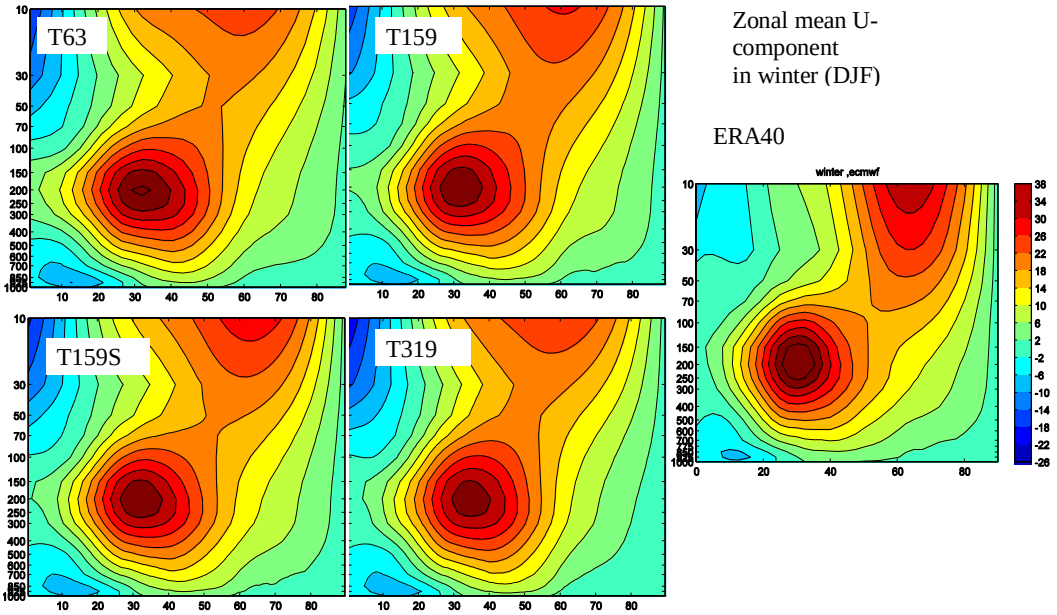

Figure 10. Zonal mean of the u-component of wind speed in winter (DJF) for the experiments and ERA40. Contour interval is 4 ms^{-1}.

The excessive westerlies in the troposphere were clearly connected to excessive thicknesses 500 – 1000 hPa in the same areas. This can also be seen in figure 12 and 13 showing zonal mean temperatures and differences to ERA40 respectively. Figure 13 thus shows a mid-tropospheric negative temperature anomaly with minimum at 60 °North at

T63 and a little bit further south in the other experiments. Better resolution removes much of the anomalies, but the thickness maps still showed excessive baroclinicity in some areas, such as upstream the Icelandic low.

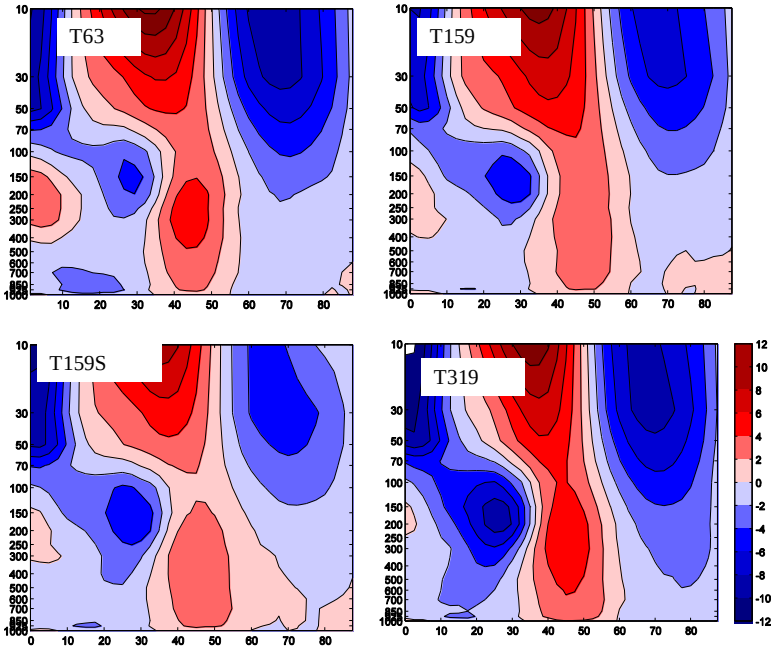

Figure 11. Difference in mean zonal u-component of the wind speed in winter (DJF) between the experiments and ERA40. Contour interval is 2 ms^{-1}.

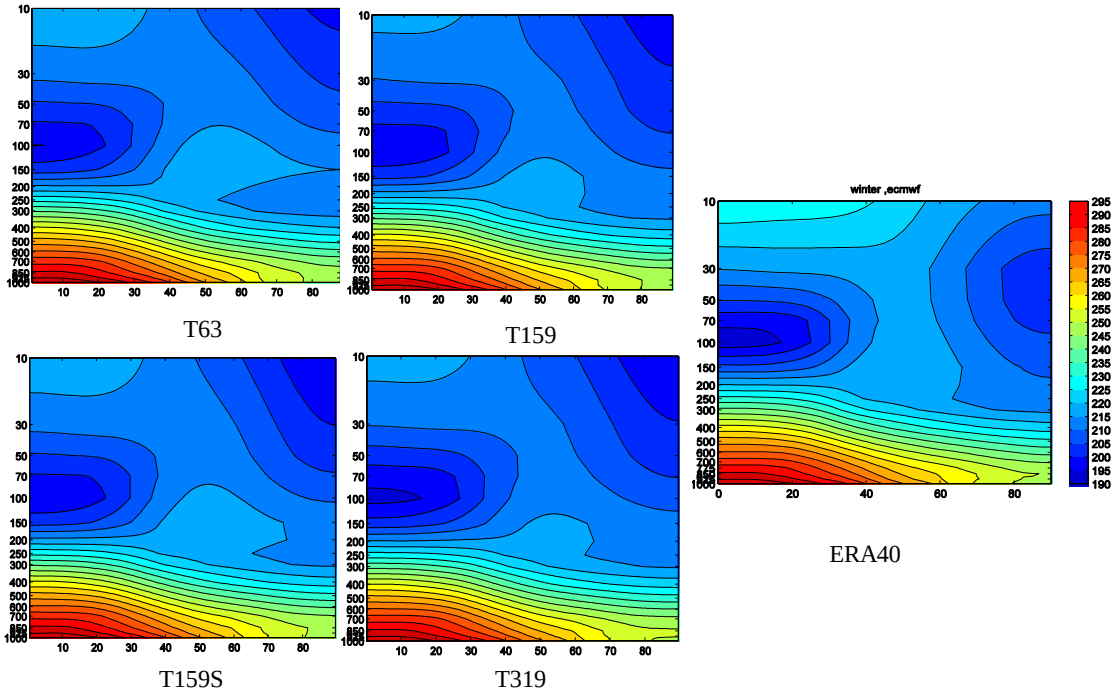

Figure 12. Zonal mean temperature in winter (DJF) for the experiments and ERA40. Contour interval is 5 K.

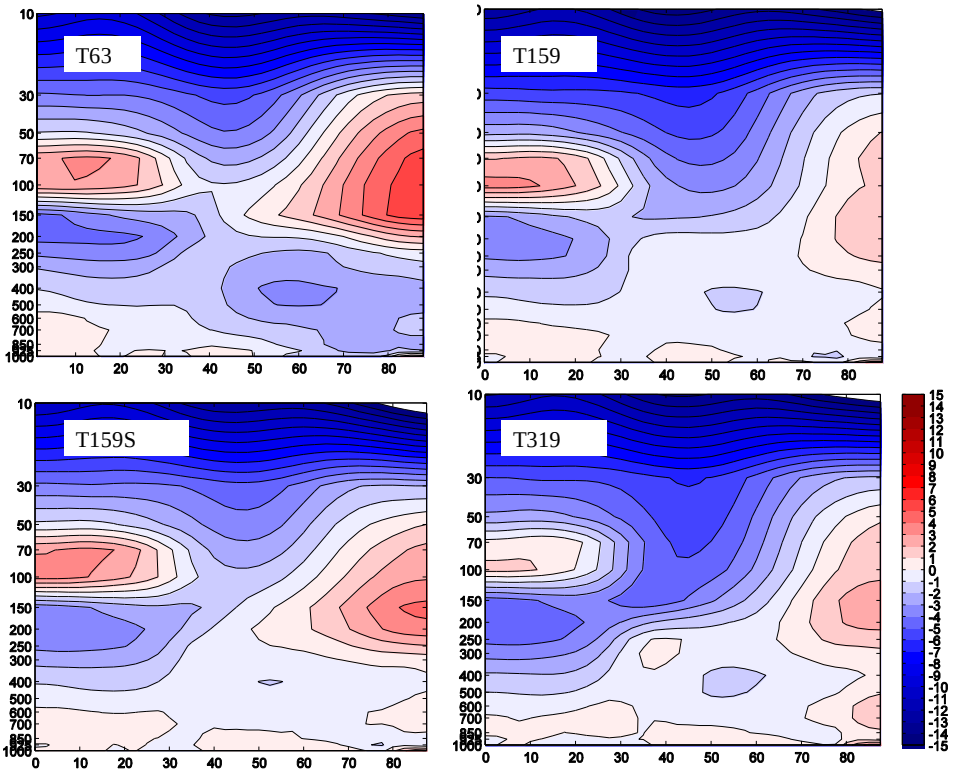

Figure 13. Difference of mean zonal temperature in winter (DJF) between the experiments and ERA40 (contour step 1 K).

While the depth of the Icelandic low was much as in ERA40 for T63, the low became considerably stronger than observed for T159 and T1319. From general experience from weather prediction models we know that mesoscale structures, like the inner core of strong extratropical cyclones, will not be sufficiently resolved in T63. Higher resolution (T159, T319) generally give far stronger and more realistic developments. Improvements, giving additional development of more than 10 hPa have been found for individual strong cyclones going from T63 to T319 (Idar Barstad, master thesis Department of Geophysics, University of Bergen, 1998). The excessive baroclinicity in our experiments will lead to stronger cyclogenesis and higher frequency of extratropical cyclones than observed. With sufficient resolution for realistic developments of individual cyclones, the Icelandic Low, formed by the sum of all cyclonic activity in the area, naturally becomes stronger than observed. With low resolution and observed baroclinicity, the Icelandic Low should become less intense than observed. In our experiments with excessive baroclinicity, naturally T159 and T319 shows a deeper Icelandic Low than observed, while T63 gets the amplitude about right for the same reason. The positioning and in particular the shape of the low was improved with better resolution. The same arguments are valid for the Aleutian Low, however, here an increase in the resolution from T159 to T319 gave a stronger increase in the intensity than for the Icelandic Low. We believe that if the error in the baroclinicity could be eliminated, high resolutions will show substantial improvements in the simulation of the Icelandic and the Aleutian Lows.

It is beyond the scope of this paper to find explanations for the errors, such as the excessive high mid-latitude baroclinicity. It could, however, be connected to the strength of the Hadley Cell. Figure 14 and 15 shows the zonal mean of the vertical velocity as expressed in pressure coodinates by ω = Dp/Dt. All the experiments have areas of mean vertical motion much as in ERA40 with rising motion just north of equator and sinking motion further north. In ERA40 maximum sinking motions is found at approximately 20 ºNorth, while in the experiments this maximum is found a little further north. It is seen from meridional temperature distribution in Figure 10 and 11 and in maps of thicknesses 500 – 1000 hPa, that excessive sinking too far north give higher temperature in the lower troposphere than in ERA40. In this way this error contributes to the excessive baroclinicity. Maximum mean rising motion in ERA40 is found at 60 ºNorth. In T63 this maximum is found 5 ° further south. This means the distribution of the vertical velocity correspond well to the increased baroclinicity and the excessive westerly wind at mid-latitudes. Better resolution gives stronger rising motion at around 60 ºNorth, but still there is too much rising motion – which contributes to a cold anomaly – between 50 and 60 ºNorth.

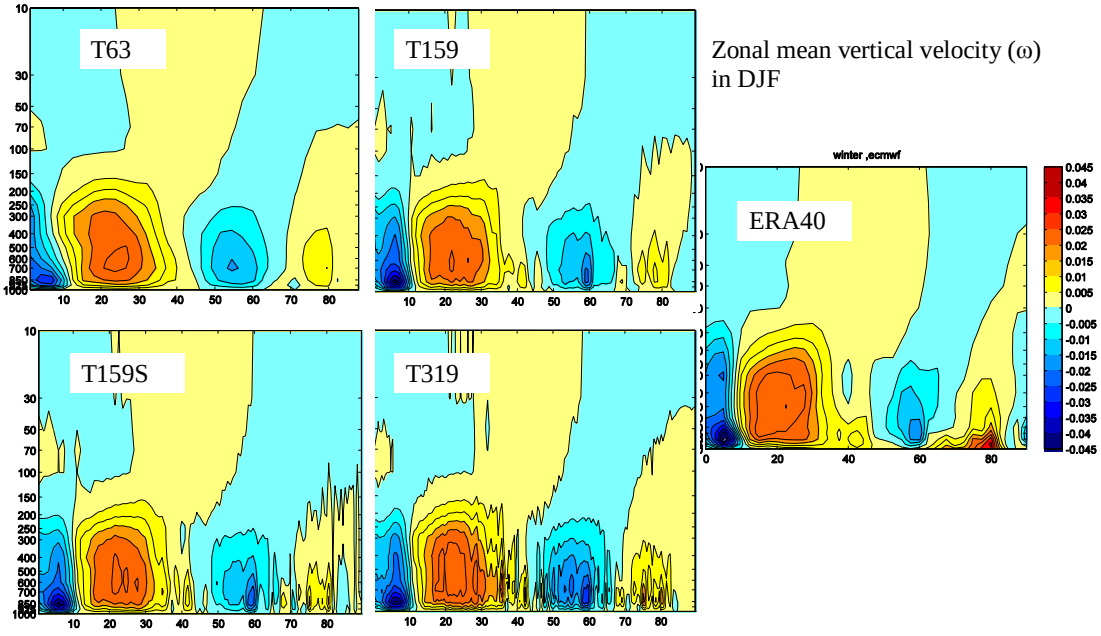

Figure 14. Zonal mean vertical velocity ω (Pas^{-1}) in winter (DJF) for the experiments and ERA40. Contour interval is 0.005 Pas^{-1}.

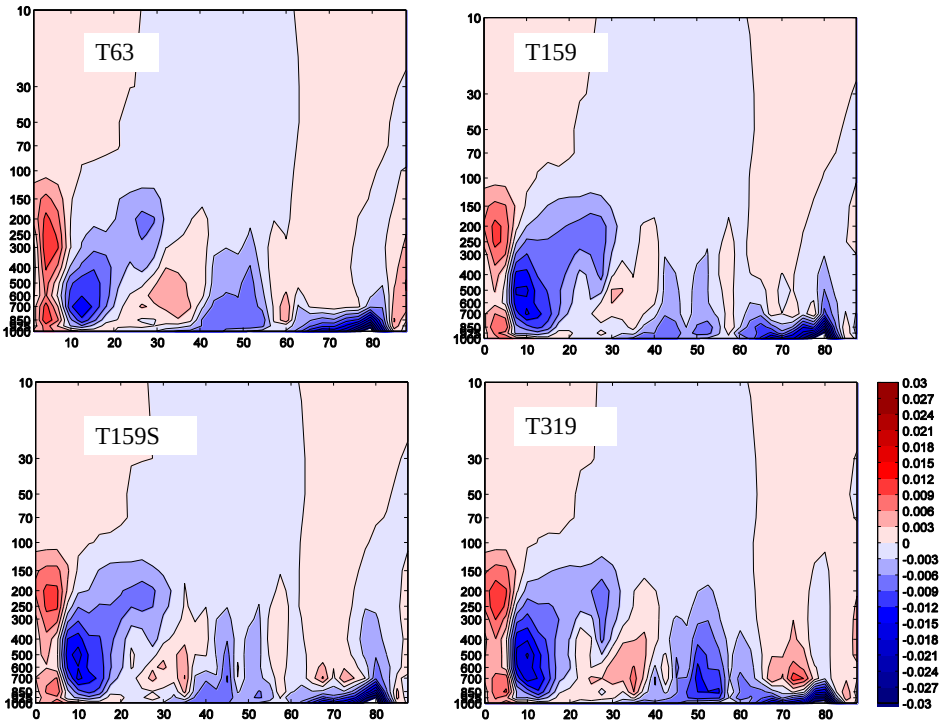

Figure 15. Difference of zonal mean vertical wind speed (ω) in winter between the experiments and ERA40. Contour interval is 0.003 Pas^{-1}.

There might be several reasons to the excessive mid-latitude baroclinicity. It might be connected to the parameterisation of deep convection in the tropics, a notorious difficult area of parameterisation. The increased mid-latitude baroclinicity contributes to the excessive westerly winds in the same area. Stronger cyclogenesis might also contribute to the strong westerly winds found at the surface in certain areas, such as over Europe. The excessive westerlies are common for several atmospheric models. It is also found in the coupled BCM (Furevik et al., 2003) an in ARPEGE (Déqué and Piedelievre,1995; Gibelin and Déqué, 2003). The problem with too strong westerlies is also believed to be related to the parameterisation of the gravity wave drag (e.g. Lott, 1994). In weather predictions models this effect is artificially strengthened in order to get the observed strength of the upper tropospheric jets. On the other hand, the circulation in the stratosphere might then be distorted. This might be acceptable for weather forecasting, but not for climate simulations. Experiments with ARPEGE have shown this sensitivity of the westerlies to the parameterisation of the gravity wave drag, in particular in mid-latitude North Atlantic (master theses by Frode Håvik Korneliussen, Department of Geophysics, University of Bergen, 2004).

The ridge over Arctic in the surface pressure, as an extension of the Sibirian High over Arctic towards the Rocky Mountains, got a better shape with higher resolution than in T63, however, the amplitude was too low all the way from the Sibirian High to the Rocky Mountains and lower than in T63. In Figure 13 all experiments show a warm bias close to the surface as a sign of an insufficient description of the Arctic inversion. In T63 the

tropospheric air is too cold over Arctic, in agreement with what we found for the thickness 500 – 1000 hPa earlier. This indicates that the high amplitude of the surface rigde in T63 is due to the cold anomaly above the inversion. For increased resolution the cold anomaly – and the surface pressure - is reduced and partly changed to small positive tropospheric anomalies in addition to those close to the surface.

The warm bias in ARPEGE in Arctic connected to the Arctic surface inversion has previously been reported by Bossuet et al. (1998). ARPEGE seems to share this systematic error with several other IPCC models (Tao et al. 1996). However, the majority of the regional models in the Arctic model intercomparison project (Tjernström et al, 2004; Rinke elt al., 2006) were found to be too cold north of 60 °N throughout the entire atmosphere. Refinement of the vertical resolution in those models is leading to a warming of the Arctic atmosphere. Byrkjedal (2006) have shown that the warm bias in ARPEGE is reduced with increased number of layers, giving a better simulation of the Arctic inversions.

Models with a warm bias obviously have difficulties to reproduce the low temperatures of the inversion. The report on Arctic climate and modelling in ACIA (2005) revealed serious discrepancy between observed and modelled geographical pattern of the Arctic climate evolution over the last 50 years. A comparison of prediction with the ECMWF weather prediction model (Beesley et al., 2000), with reliable data during the SHEBA experiment (Uttal et al., 2002), showed that the model systematically lost the extremes in surface temperatures. The model seemed to produce too much mechanical mixing in such cases. In case of warm air advection the surface air was found to respond too quickly. A warm bias resulted. Similar results were found by Kiehl and Gent, 2004) for the NCAR model CCSM-2. Recent intercomparisons by Cuxart et al. (2006) traced some of the problem to excessive turbulent fluxes. Most models use constraints on the minimum possible flux (Beljaars and Viterbo, 1999) in order to prevent decoupling of the boundary layer, which might give model instabilities.

We propose that the warm bias above the Arctic inversion in our experiments with higher resolution is connected with a shallower inversion than observed. From weather forecasting based on weather prediction models we know that warm air from south climb the inversions nearly as they were mountains (Grønås, personal communication). ERA40 also show mean rising motion close to the pole. When the simulated inversions are too shallow, the "mountain" becomes lower than observed. In this way the positive vertical velocities become too small, resulting in less cooling than observed. This seems to be in accordance with the weak – mainly positive – mean vertical velocity in all the experiments.

The storm track activity in T63 was found to be less than in ERA40. This is in agreement with Lambert and Fyfe (2006), who found that the AOGCMs participating in the IPCC AR4 exercise – with resolutions around that of T63 - tend to underestimate the number of extratropical cyclones. The storm tracks were improved in T159, T319 and T159S compared to tracks in T63. Higher resolution increased the cyclone activity, in particular higher activity up the Norwegian Sea towards the Barents Sea and in Arctic. The

improvements are in accordance with similar improvements in the distribution of sea level pressure with respect to the extension of the Icelandic Low toward the Barents Sea. Even with the highest resolution, there is still too much cyclone activity towards northern Europe on the expense of too little activity in the Norwegian Sea. We believe that is a consequence of the excessive upstream baroclinicity. Results from AMIP II simulations (PCMDI, 2004) indicates that the problem with stronger westerlies and more zonally directed mid-latitude storm tracks than observed, is a problem shared by several climate models.

We have shown how increased resolution beyond that in T63 has affected the systematic error in the main pressure structures and in the storm tracks. In several ways better resolution reduced the systematic errors. In particular, the improvement going from T63 to T159 was evident. Nevertheless, some errors became more serious as resolution was increased. The reason for the deterioration might be connected to some weaknesses of the physical parameterisation in the model – such as deep convection in the tropics, boundary layer physics of the Arctic - become more apparent as the resolution is increased. We hope that the resolution in BCM will be increased for the atmospheric part to give an appropriate representation of extratropical cyclones. Efforts to improve the physical parameterisation of ARPEGE must be central in such efforts.

The experiment with stretched coordinates, focussing the resolution in Arctic, gave promising results. The improvements seen in e.g. surface pressure and storm track connected to Northern Europe and Arctic with highest resolution, was also seen in T159S. Indeed, in several ways T159S showed to best results with respect to structures like the Icelandic and the Aleutian Lows. However, it should be born in mind that this result might have been obtained for wrong reasons (see discussion above).

4. Downscaling of wind and precipitation

We have so far concentrated on the systematic errors in principle fields of the troposphere and storm tracks. The main purpose of downscaling is to simulate the climate of parameters more directly connected to local weather such as temperature, precipitation and surface wind. We know that even the resolution in T319 is too course to describe climate variations in mountainous terrain like that in Norway. Where surface observations exist, empirical downscaling based on the results from dynamical downscaling is possible for estimation of local weather and climate.

Naturally, extreme weather has a particular interest, and we will here just demonstrate how extreme surface wind and precipitation accumulated over 24 hours vary with resolution, concentrating on areas covering the Norwegian and the Barents Sea and surrounding land areas. We will evaluate the results according what is known about extreme wind and precipitation in the area.

Maximum wind and precipitation during the integrations are picked out for each grid point and the results are presented for the mentioned area in Figure 16 and 17. Output every 6 hours has been used.

Wind

Figure 16 shows the maximum wind at 925 hPa in the experiments during the total integrations for an area covering the Norwegian and Barents Sea. We have chosen to use this pressure layer instead of the wind at 10 m which might have been more appropriate. The wind at 10 m is, however, a derived diagnostic result from the dependent variables in the model levels and the computations might contain additional errors. We have chosen 925 hPa, partly because mountainous effects of mountain ranges like the Scandinavian mountains, will be noticeable.

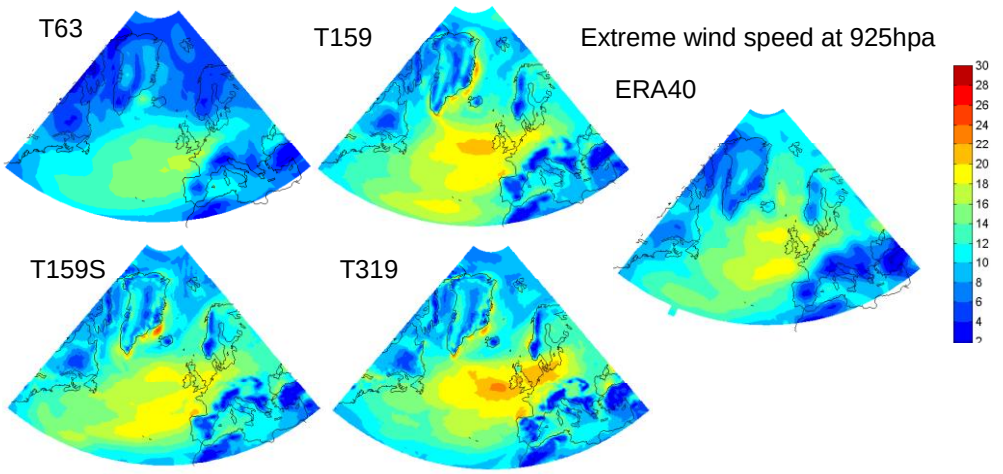

Figure 16. Extreme wind speed at 925 hPa at each grid point for the experiments and ERA40. Contour interval is 2ms^{-1}.

The variation of the extreme winds in the area with resolution demonstrates the need for high resolution in order to describe extreme weather. This is illustrated by the fact that maximum wind in ERA40 is 21 ms^{-1} in Figure 16, while the strongest wind in T319 is 30 ms^{-1}. The distribution of the extreme wind in T319 contains several structures that are missing in ERA40, but well known from weather forecasting.

Both ERA40 and T319 show a decrease in maximum wind from the storm track areas south of Iceland towards the Barents Sea. This is in accordance with other investigations (Eirik Kolstad, personal communication and Norwegian investigations for the oil industry). This decrease is probably too strong in T319 since the storm activity is less than observed.

T319 clearly shows some areas of strong wind connected to mountains, but not present in ERA40. We find a belt of strong wind on the western side of southern Norway which is in accordance with observations and theoretical considerations (Barstad and Grønås, 2005; 2006). The maximum wind here is southwesterly or westerly and stronger than the maximum winds in the storm tracks over the ocean. This is also in accordance with general weather prediction experience in the area. The very strongest winds are found east of Greenland. Here the associated wind direction is from north. Such winds have

been named barrier winds (Moore and Renfrew 2005), indicating that the steep slopes of Greenland acts as a barrier for northerly flows.

Even with the resolution of T319, some known strong winds are not resolved. Strong winds south of Spitsbergen in flows east and northeast (Skeie and Grønås, 1999) are not resolved. In addition, the resolution is not sufficient for describing hurricane force wind at the marginal ice zone and in Arctic fronts that frequently is found over the sea downstream from the ice (Grønås and Skeie, 1999).

Precipitation

There are large variations in the level of extreme precipitation between the experiments (Figure 17). The main change takes place going from T63 to T159. While there in T63 are small signs of orographic precipitation, T159 show orographic precipitation in areas known for extensive orographic precipitation, such as western Norway and southeastern Greenland. Naturally, a further increase in the resolution gives even stronger orographic precipitation. We also find a substantial increase in extreme precipitation in the main storm track areas. Higher resolution give more strong precipitation in the area south of Iceland and also up the eastern part of the Norwegian Sea. This increase illustrates both an effect in changes in the storm tracks discussed earlier and stronger vertical circulation with increased resolution.

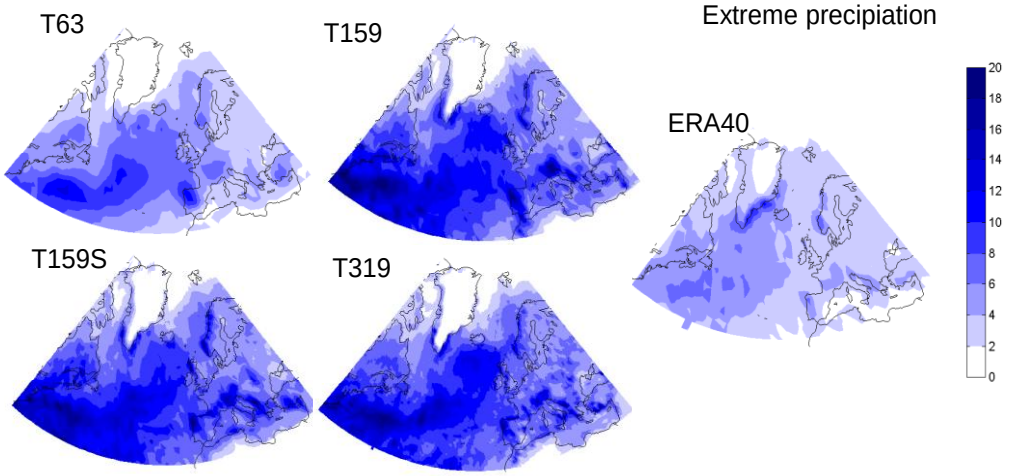

Figure 17. Extreme precipitation at each grid point for the experiments and ERA40. Contour interval is 2 mmday^{-1}.

Extreme precipitation is modest in ERA40. This partly related to the course resolution available for the data. However, ERA40 shows sign of orographic precipitation. Since the precipitation is produced by a short range forecast with the ECMWF model, the small amounts could also be connected to spin-up problem in the model. While all our experiments show very small amounts over sea ice in Artic and over high mountains of Greenland, the amounts are significantly higher in ERA40.

5. Concluding remarks

In this paper AMIP kind of experiments on present day climate have been made with the global atmospheric model ARPEGE with horizontal resolution varying from T63 to T319. Vertically, there were 31 layers in all the experiments. The impact of higher horizontal resolution on the general circulation of northern mid and high latitudes has been evaluated against analyses in ERA40, concentrating on the winter season and principle parameters, such as the sea level pressure and height of the 500 hPa surface, and storm tracks.

It has been shown that an increase in the horizontal resolution from T63 to T159 improves the general circulation in the area investigated. The structure of the Icelandic and Aleutian Lows is improved, in particular the extension of the Icelandic Low over the Norwegian Sea towards the Barents Sea. The storm tracks, evaluated from band-passed standard deviations related to extratropical cyclones, are also improved and in accordance with the improvements in the mean structures. In particular, the storm tracks in Arctic and towards Arctic become more realistic. The main reason for the improvements seems to be that individual cyclones are better resolved with T159 than with T63. Further increase in the resolution to T319 gives some further improvements, primarily in flows over mountains like Greenland. Nevertheless, the main progress was achieved going from T63 to T159.

The experiments clearly demonstrated that some weaknesses in ARPEGE become more apparent when the resolution is increased. Compared to the reanalyses ERA40, the model showed excessive mid-latitude baroclinicity in all the experiments, e.g. upstream of the Icelandic Low. Better resolution of the individual cyclones resulted in too deep mean low systems, in particular the Icelandic Low. The strengthened baroclinicity naturally also contributed to stronger mid-latitude jets than in ERA40 and excessive storm tracks towards northern Europe on the expense of too little activity up the Norwegian Sea. However, better resolution gave some improvements in the excessive westerlies and in the storm tracks in the area.

The problem with the excessive baroclinicity and too strong westerly winds is probably very complex. We have suggested that it might be connected to errors in the Hadley Cell, giving too high tropospheric temperatures in sub-tropics. The error could also be connected to the parameterisation of sub-scale gravity wave drag. Our experiments have been performed with version 3 of ARPEGE. A version 4 is now made available by Meteo-France. BCCR has made an additional experiment with this version (T63). The problem with the excessive baroclinicity seems to remain, however.

Increased resolution improved the structure and the shape of the Arctic Ridge extending from the Siberian High over Arctic towards the ridge over Rocky Mountains. In addition the variability, as expressed by band-passed filtered standard deviations focussed on synoptic activity, was increased and improved. Nevertheless, a warm bias in Arctic was found causing too low amplitudes of the ridge. Some of the errors were found to be due to problems with the inversions and surface temperatures, some was due to a warm bias

in tropospheric layers above the inversions. We have suggested that the latter bias might also be a consequence of the problems with Arctic inversions.

Focussing the resolution in Arctic using the stretched version T159S gave satisfactorily results compared to results with uniform high resolution (T319). The storm tracks towards northern Europe and the Norwegian Sea was at least as correct as with T319. One reason for the success was probably that the stretching gave sufficient resolution in the Northern Atlantic to resolve individual cyclones, i.e. resolution T159 or more.

The ability of the atmospheric model to represent extreme wind close to the surface and extreme precipitation was investigated. The results showed, as expected, an increasing ability to describe extremes with increasing resolution. High resolution is necessary to describe the mountains in some detail and the mountain flow. Only the highest resolution (T319 and T159S) descibed known extreme wind connected to topographic effects of Scandinavia and Greenland. Ororgraphic precipitation was found for all resolutions, but considerably more realistically for the highest resolution (T319). Even the best resolution shows systematic errors compared to observed wind and precipitation (direct measurement). Empirical downscaling of the dynamically downscaled weather parameters is recommended to describe sub-scale effects.

We have demonstrated that downscaling using a global atmospheric climate model gives improvements in the general circulation of the atmosphere compared to results obtained in the coupled climate models BCM with lower resolution. In this respect we have shown that downscaling with an AGCM has an advantage compared to downscaling with a RCM. We have also demonstrated that downscaling using stretched coordinates focussing on Arctic might be a beneficial alternative to high uniform resolution. It should however be born in mind that the main climate information in dynamical downscaling is held in the results from the coupled climate model itself. For successful downscaling of climate projections for Arctic with a global atmospheric model, this means that the coupled model must be able to simulate a reliable representation of the sea-ice and the SSTs in the area. In the case of BCM and several other present day climate models without use of flux correction, this is not the case. For instance, BCM has severe problems with the sea-ice in the Barents Sea. Downscaling of such results for Arctic is certainly questionable and might have little meaning. Furthermore, we have demonstrated, along with previous results summarised in ACIA (2005), considerable systematic errors for Arctic in high resolution experiments with an atmospheric model with observed SST and sea-ice. The current situation, with models having problems with the sea-ice and Arctic inversions, might call for dynamical downscaling for Arctic with coupled models along the line of attack summarised in Section 2. However, the main goal to improve the global climate models with respect to resolution and physical parameterisation of the atmospheric part, should always be underscored. Hopefully, efforts to improve the coupled models and efforts to improve dynamical downscaling will be to parts of the same research activity.

6. Acknowledgement

This computer time for the experiments was provided by the Research Council of Norway.

References

Antic, S., R. Laprise, B. Denis and R. de Elia, 2005: Testing the downscaling ability of a one-way nested regional climate model in regions of complex topography. Climate Dynamics, 23, 473-493.

Barry R. G. and A. M. Carleton: Synoptic and dynamic climatology. American meteorological society, 2001.

Beesley, T. A., C. S. Bretherton, C. Jakob, E. L Andreas, J. M. Intrieri, and T. A. Uttal, 2000: A comparison of cloud and boundary layer variables in the ECMWF forecast model with observations at Surface Heat Budget of the Arctic Ocean (SHEBA) ice camp, J. Geophys. Res., 105(D10), 12337-12350

Beljaars, A.C.M. and Viterbo P., 1999: The role of the boundary layer in a numerical weather prediction model, in: Clear and cloudy boundary layers, A.A.M. Holtslag and P.G. Duynkerke (eds.), North Holland Publishers.

Bengtsson L. , V. A. Semenov and O. M. Johannessen, 2004: The Early Twentieth-Century Warming in the Arctic—A Possible Mechanism. *Journal of Climate*, 17, 4045–4057.

Blackmon M. L., 1976: A Climatological Spectral Study of the 500 mb Geopotential Height of the Northern Hemisphere. *Journal of the Atmospheric Sciences*, 33, 1607–1623.

Bleck R., C. Rooth, D. Hu and L. T. Smith, 1992: Salinity-driven thermocline transients in a wind- and thermohaline-forced isopycnic coordinate model of the North Atlantic. J. Phys. Oceanogr, 22, 1486-1505

Blenckner T, and Chen D (2003) Comparison of the impact of regional and North-Atlantic atmospheric circulation on an aquatic ecosystem. Clim Res 23:131-136

Boer, G.J., 2000a: Analysis and verification of model climate. In: P. Mote and A. O'Neill (eds.). Numerical Modeling of the Global Atmosphere in the Climate System. NATO Science Series C-550. Kluwer Academic Publishers.

Boer, G.J., 2000b: Climate model intercomparison. In: P. Mote and A. O'Neill (eds.). Numerical Modeling of the Global Atmosphere in the Climate System. NATO Science Series C-550. Kluwer Academic Publishers.

Bogdanova E. G. , B. M. Ilyin and I. V. Dragomilova, 2002: Application of a Comprehensive Bias-Correction Model to Precipitation Measured at Russian North Pole Drifting Stations. *Journal of Hydrometeorology*, 3, 700–713.

Cannon, A., and P. Whitfield, 2002: Downscaling recent streamflow conditions in British Columbia, Canada using ensemble neural network models. Journal of Hydrology, 259(1-4), 136-151.

Caya, D., and S. Biner, 2004: Internal variability of RCM simulations over an annual cycle. Climate Dynamics, 22, 33-46.

Chang, E.K.M., S. Lee, and K.L. Swanson, 2002: Storm track dynamics. *J. Climate*, **15**, 2163-2183.

Chang, E. K. M., and I. Orlanski, 1993: On the dynamics of a storm track. *Journal of the Atmospheric Sciences*, 50(7), 999-1015.

Debernard, J., M.Ø. Køltzow, J.E. Haugen, and L.P. Røed, 2003: Improvements in the sea-ice module of the regional coupled atmosphere-ice-ocean model and the strategy for the coupling of the three spheres. In: RegClim General Technical Report No. 7 [T. Iversen and M. Lystad (eds)], Norwegian Meteorological Institute, P.O.Box 43, Blindern, N-0313 Oslo, Norway, pp. 59-69.

Denis B., J. Côté and R. Laprise, 2002: Spectral Decomposition of Two-Dimensional Atmospheric Fields on Limited-Area Domains Using the Discrete Cosine Transform (DCT). *Monthly Weather Review*, 130, 1812–1829.

Dethloff, K., C. Abegg, A. Rinke, I. Hebestad, and V. Romanov, 2001: Sensitivity of Arctic climate simulations to different boundary layer parameterizations in a regional climate model, Tellus, 53, 1-26.

Déqué M., C. Dreveton, A. Braun and D. Cariolle, 1994: The ARPEGE/IFS atmosphere model- a contribution to the French Community Climate Modeling. *Clim. Dyn.*, 10, 249-266.

Déqué, M., and J. P. Piedelievre, 1995: High resolution climate simulation over Europe. Climate Dynamics, 11, 321-339

Déqué M., P. Marquet, and R. G. Jones, 1998: Simulation of climate change over Europe using a global variable resolution general circulation model. *Clim. Dyn*., 14, 173-189.

Déqué, M., and A. L. Gibelin, 2002: High versus variable resolution in climate modelling. Research Activities in Atmospheric and Oceanic Modelling, (Ed. Hal Ritchie), WMO/TD – No 1105, Report No. 32, 74-75.

Dickinson, R. E., R. M. Errico, F. Giorgi and G. T. Bates, 1989: A regional climate model for western United States. Climate Change, 15, 383-422.

Dimitrijevic, M., and R. Laprise, 2005: Validation of the nesting technique in a Regional Climate Model through sensitivity tests to spatial resolution and the time interval of lateral boundary conditions during summer. Climate Dynamics. , 25, 555-580.

Douville H., 2005: Limitations of time-slice experiments for predicting regional climate change over South Asia. *Clim. Dyn.*, 24, 373-391, DOI: 10.1007/s00382-004-0509-7.

Döscher, R., U. Willen, C. Jones, A. Rutgersson, H. Meier, and U. Hansson, 2002: The development of the coupled ocean-atmosphere model RCAO. Boreal Environmental Research, 7, 183-192.

Drange H, 1999: RegClim ocean modeling at NERSC. In: RegClim general technical report No. 2, pp 93-102. Norwegian Institute for Air Research, Kjeller, Norway

Duffy, P.B., B. Govindasamy, J.P. Iorio, J. Milovich, K.R. Sperber, K.E. Taylor, M.F. Wehner and S.L. Thompson, 2003: High-resolution simulations of global climate, part 1: Present climate, Climate Dynamics, 21, 371-390

Fox-Rabinovitz M. S. , L. L. Takacs, R. C. Govindaraju and M. J. Suarez, 2001: A Variable-Resolution Stretched-Grid General Circulation Model: Regional Climate Simulation. *Monthly Weather Review*: Vol. 129, No. 3, pp. 453–469.

Furevik,T., M. Bentsen, H. Drange, I.K.T. Kindem, N.G. Kvamstø and A. Sorteberg, 2003. Description and validation of the Bergen Climate Model: ARPEGE coupled with MICOM. Climate Dynamics, 21:27–51.

Gao, Q., and M. Yu, 1998: A model of regional vegetation dynamics and its application to the study of Northeast China Transect (NECT) responses to global change. Global Biogeochemical Cycles, 12(2), 329-344.

Gibelin, A. L., and Déqué, M., 2003: Anthropogenic climate change over the Mediterranean region simulated by a global variable resolution model. Clim. Dyn. 20, 327-339

Giorgi F. and G. T. Bates, 1989: The Climatological Skill of a Regional Model over Complex Terrain. *Monthly Weather Review*, 117, 2325–2347.

Goodison, B.E., P.Y.T. Louie, and D. Yang, 1998: WMO solid precipitation measurement intercomparison, final report. WMO/TD-No.872, WMO, Geneva, 212pp.

Govindasamy, B., K. Caldeira and P.B. Duffy, 2003: Geoengineering Earth's radiation balance to mitigate climate change from a quadrupling of CO_2. Global and Planetary Change, 37(1-2), 157-168.

Hansen, J., Mki. Sato, R. Ruedy, K. Lo, D.W. Lea, and M. Medina-Elizade 2006: Global temperature change. Proc. Natl. Acad. Sci. 103, 14288-14293, doi:10.1073/pnas.0606291103.

Hoskins B. J. and K. I. Hodges, 2002: New Perspectives on the Northern Hemisphere Winter Storm Tracks. *Journal of the Atmospheric Sciences*: Vol. 59, No. 6, pp. 1041–1061.

Hoskins B. J. and P. J. Valdes, 1990: On the Existence of Storm-Tracks. *Journal of the Atmospheric Sciences*: Vol. 47, No. 15, pp. 1854–1864.

Hurrell, J. W., 1995: Decadal trends in the North Atlantic Oscillation: regional temperatures and precipitation. *Science*, 269: 676-679.

Inatsu, M. and M. Kimoto, 2005: Difference of boreal summer climate between coupled and atmosphere-only GCMs. Scientific Online Letters on the Atmosphere, 1, 105-108.

IPCC, 2001. Climate Change 2001: The Scientific Basis. Contribution of Working Group I to the Third Assessment Report of the Intergovernmental Panel on Climate Change. J.T. Houghton, Y. Ding, D.J. Griggs, M. Noguer, P.J. van der Linden, X. Dai, K. Maskell and C.A. Johnson (eds.). Intergovernmental Panel on Climate Change. Cambridge University Press, Chapter 10, Appendix 10.4

Johannessen, O. M., L. Bengtsson, M. W. Miles, S. I. Kuzmina, V. A.Semenov, et al., 2004. Arctic climate change – observed and modelled temperature and sea ice. *Tellus* 56A, 328–341.

Jones, R.G., J.M. Murphy, M. Noguer and A.B. Keen, 1997: Simulation of climate change over Europe using a nested regional climate model. II: Comparison of driving and regional model responses to a doubling of carbon dioxide. Quart. J. Roy. Met. Soc., 123, 265–292.

Kanada, S., C. Muroi, Y. Wakazuki, K. Yasunaga, A. Hashimoto, T. Kato, K. Kurihara, M. Yoshizaki and A. Noda, 2005: Structure of Mesoscale Convective Systems during the Late Baiu Season in the Global Warming Climate Simulated by a Non-Hydrostatic Regional Model, SOLA, 1, 117-120

Kiehl, J. T., and P. R. Gent, 2004: The Community Climate System Model, version two. *Journal of Climate*, 17, 3666-3682.

Lambert, S. and J.C. Fyfe, 2006: Changes in winter cyclone frequencies and strengths simulated in enhanced greenhouse gas experiments: Results from the models participating in the IPCC diagnostic exersize. Climate Dynamics, 26, 713-728

Lee, W-J., and M. Mak, 1996: The Role of Orography in the Dynamics of Storm Tracks, *J. Atmos. Sci.*, 53, 1737-1750.

Liu, J., J.A. Curry, W.B. Rossow, J.R. Key, and X. Wang, 2005: Comparison of surface radiative flux data sets over the Arctic Ocean. J. Geophys. Res., 110, C02015, doi: 10.1029/2004JC002381

Lorenz, P, and D. Jacob, 2005: Influence of regional scale information on the global circulation: A two-way nesting climate simulation. Geophys. Res. Lett., VOL. 32, L18706, doi:10.1029/2005GL023351, 2005

Lott, F., 1994: The significance of subgrid scale orography and problems in their representation in GCM, in Parametrization of sub-grid scale physical processes, Seminar Proceedings, 277--303, ECMWF

Maslanik J. A. , A. H. Lynch, M. C. Serreze and W. Wu, 2000: A Case Study of Regional Climate Anomalies in the Arctic: Performance Requirements for a Coupled Model. *Journal of Climate*, 13, 383–401.

May, W. and E. Roeckner, 2001: A time-slice experiment with the ECHAM4 AGCM at high resolution: The impact of horizontal resolution on annual mean climate Change. Climate Dynamics, 17, 407-420.

McGregor, J. L., K. C. Nguyen and J. J. Katzfey, 2002: Regional climate simulations using a stretched-grid global model. Research Activities in Atmospheric and Oceanic Modelling. [Ritchie, H. (ed.)]. Report No. 32 WMO/TD- No. 1105, 3.15-16.

Meier, H.E.M., R. Döscher and A. Halkka, 2004: Simulated distributions of Baltic sea-ice in warming climate and consequences for the winter habitat of the Baltic Sea ringed seal. Ambio, 33, 249-256.

Mikolajewicz, U., D.V. Sein, D. Jacob, T. Kahl, R. Podzun, and T. Semmler, 2005: Simulating Arctic sea ice variability with a coupled regional atmosphere-ocean-sea ice model. Meteorol. Z., 14, 793-800, doi: 10.1127/0941-2948/2005/0083.

Orlanski, I., and J. J. Katzfey, 1991: The life cycle of a cyclone wave in the Southern Hemisphere. Part I: Eddy energy budget. *Journal of the Atmospheric Sciences*, 48(17), 1972-1998.

Pan, Z., E.S. Takle and F. Otieno., 2001: Evaluation of uncertainties in regional climate change simulations. Journal of Geophysical Research, 106(D16), 17735-17752

Räisänen, J., 2002: CO_2-induced changes in interannual temperature and precipitation variability in 19 CMIP2 experiments. Journal of Climate, 15, 2395-2411

Rinke, A. and K. Dethloff, 2000: On the sensitivity of a regional Arctic climate model to initial and boundary conditions. Climate Research, 14(2), 101-113.

Rinke, A., R. Gerdes, K. Dethloff, T. Kandlbinder, M. Karcher, F. Kauker, S. Frickenhaus, C. Koeberle, and W. Hiller, 2003: A case study of the anomalous Arctic sea ice conditions during 1990: Insights from coupled and uncoupled regional climate model simulations, Journal of Geophysical Research, 108, 4275, doi: 10.1029/2002JD003146.

Rinke, A., K. Dethloff, J. Cassano, J.H. Christensen, J.A. Curry, P. Du, E. Girard, J.E. Haugen, D. Jacob, C. Jones, M. Koltzow, R. Laprise, A.H. Lynch, S. Pfeifer, M.C. Serreze, M.J. Shaw, M. Tjernstrom, K. Wyser, and M. Zagar, 2006: Evaluation of an ensemble of Arctic regional climate models: Spatial patterns and height profiles. Clim. Dyn., doi: 10.1007/s00382-005-0095-3.

Rummukainen, M., S. Bergström, G. Persson, J. Rodhe and M. Tjernström, 2004: The Swedish Regional Climate Modelling Programme, SWECLIM: a review. Ambio, 33, 176-182.

Schrum C., Hübner U., Jacob D., Podzun R. 2003, A coupled atmosphere/ice/ocean model for the North Sea and the Baltic Sea Climate Dynamics, 21, 131-151

Semmler T., D. Jacob, K. H. Schlünzen and R. Podzun, 2005: The Water and Energy Budget of the Arctic Atmosphere. *Journal of Climate*: Vol. 18, No. 13, pp. 2515–2530.

Serreze, M.C., and C.M. Hurst, 2000: Representation of mean Arctic precipitation from NCEP- NCAR and ERA reanalyses. Journal of Climate 13, 182-201.

Staniforth, A., 1997: Regional modeling: A theoretical discussion, Meteorology and Atmospheric Physics, 63,15-29.

Stott P. A. , G. S. Jones, J. A. Lowe, P. Thorne, C. Durman, T. C. Johns and J.-C. Thelen, 2006a: Transient Climate Simulations with the HadGEM1 Climate Model: Causes of Past Warming and Future Climate Change. *Journal of Climate*, 19, 2763–2782.

Stott P. A., J. F. B. Mitchell, M. R. Allen, T. L. Delworth, J. M. Gregory, G. A. Meehl and B. D. Santer, 2006b: Observational Constraints on Past Attributable Warming and Predictions of Future Global Warming. *Journal of Climate*, 19, 3055–3069.

Tao X., J. E. Walsh and W. L. Chapman, 1996: An Assessment of Global Climate Model Simulations of Arctic Air Temperatures. *Journal of Climate*: Vol. 9, No. 5, pp. 1060–1076.

Terray L, O. Thual, S. Belamari, M. Déqué, P. Dandin, C. Lévy and P. Delecluse, 1995: Climatology and interannual variability simulated by the arepege-opa model. Climate Dynamics, 11, 487-505

Tjernström, M., M. Zagar, G. Svensson, J. Cassano, S. Pfeifer, A. Rinke, K. Wyser, K. Dethloff, C. Jones, and T. Semmler, 2005: Modeling the Arctic boundary layer: An evaluation of six ARCMIP regional-scale models with data from the SHEBA project, Boundary-Layer Meteorology, 117, 337-381, doi: 10.1007/s10546-004-7954-z

Uttal T. and coauthers, 2002: Surface Heat Budget of the Arctic Ocean. *Bulletin of the American Meteorological Society*: Vol. 83, No. 2, pp. 255–275.

Vidale, L., D. Lüthi, C. Frei, S. I. Seneviratne and C. Schär, 2003: Predictability and uncertainty in a regional climate model. Journal of Geophysical Research, 108(D18), 4586, doi:10.1029/2002JD002810,2003.

Wallace, J. M. and M. L. Blackmon, 1983: Observations of low-frequency atmospheric variability. *Large-Scale Dynamical Processes in the Atmosphere*, B. J. Hoskins and R. P. Pearce, Eds., Academic Press, 55–94.

Warner T. T. , Ralph A. Peterson and Russell E. Treadon. 1997: A Tutorial on Lateral Boundary Conditions as a Basic and Potentially Serious Limitation to Regional Numerical Weather Prediction. *Bulletin of the American Meteorological Society*: Vol. 78, No. 11, pp. 2599–2617.

Wei H. , W. J. Gutowski Jr., C. J. Vorosmarty and B. M. Fekete, 2002: Calibration and Validation of a Regional Climate Model for Pan-Arctic Hydrologic Simulation. *Journal of Climate*: Vol. 15, No. 22, pp. 3222–3236.

Wyser, K., and C.G. Jones, 2005: Modeled and observed clouds during Surface Heat Budget of the Arctic Ocean (SHEBA), J. Geophys. Res., 110, D09207, doi: 10.1029/2004JD004751.

Xue, M., K.K. Droegemeier, V. Wong, 2000: The Advanced Regional Prediction System (ARPS) - A multi-scale nonhydrostatic atmospheric simulation and prediction model. Part I: Model dynamics and verification. Meteorology and Atmospheric Physics, 75(3 – 4), 161-193.

Yoshizaki, M., C. Muroi, S. Kanada, Y. Wakazuki, K. Yasunaga, A. Hashimoto, T. Kato, K. Kurihara, A. Noda and S. Kusunoki, 2005: Changes of Baiu (Mei-yu) frontal activity in the global warming climate simulated by a non-hydrostatic regional model. SOLA, 1, 25-28.